CHARACTERIZATION OF THE TYPE III EFFECTOR VOPA
FROM *VIBRIO PARAHAEMOLYTICUS*

APPROVED BY SUPERVISORY COMMITTEE

Kim Orth, Ph.D. _____

Vanessa Sperandio, Ph.D., Chair _____

Paul Blount, Ph.D. _____

Lora Hooper, Ph.D. _____

DEDICATION

To my parents, Jim and Paula Trosky who always encouraged me to follow my dreams.
To my brothers, Zac and Ian and my sister, Samantha for always being there when I needed someone to lean on.

To my husband Horácio Dinalo who was not there in the beginning but who has been a pillar of support in the end.

I would also like to thank my mentor Kim Orth for her support and encouragement in the bad times and her enthusiasm during the good times. I would also like to thank my committee member, Drs. Vanessa Sperandio, Lora Hooper and Paul Blount for their helpful discussion and encouragement. Many thanks to all of the members of the Orth lab who have made it such a fun place to work. Also to all my friend and colleagues at UT Southwestern who have made my experience here such a great one.

CHARACTERIZATION OF THE TYPE III EFFECTOR VOPA FROM *VIBRIO PARAHAEMOLYTICUS*

by

JENNIFER E. TROSKY

DISSERTATION

Presented to the Faculty of the Graduate School of Biomedical Sciences

The University of Texas Southwestern Medical Center at Dallas

In Partial Fulfillment of the Requirements

For the Degree of

DOCTOR OF PHILOSOPHY

The University of Texas Southwestern Medical Center at Dallas

Dallas, Texas

September, 2007

CHARACTERIZATION OF THE TYPE III EFFECTOR VOPA FROM *VIBRIO PARAHAEMOLYTICUS*

Publicaton No. _____

Jennifer E. Trosky

The University of Texas Southwestern Medical Center at Dallas, 2007

Supervising Professor: Kim Orth, Ph.D.

Vibrio parahaemolyticus is a marine bacterium and causative agent of gastroenteritis associated with the consumption of contaminated seafood. It is endemic to Southeast Asia and is the leading cause of gastroenteritis in Japan. Sequencing of the *Vibrio parahaemolyticus* genome revealed the presence of a type III secretion system (TTSS) encoded within a pathogenicity island. Within

this pathogenicity island a homologue of the *Yersinia* type III effector YopJ was found and is referred to as VopA (*Vibrio* outer protein A). The founding member of the family, YopJ from *Yersinia spp.,* inhibits the MAPK and the NFκB signaling cascades within the host cell, thereby inhibiting the host's innate immune response. Recently our lab elucidated the mechanism of YopJ's inhibition by demonstrating that YopJ acetylates MKKs and inhibits kinase activation by blocking phosphorylation (1).

The molecular characterization of VopA has focused on its effect on signaling pathways. In contrast to YopJ, VopA only inhibits MAPK signaling and shows no effect on the NFκB pathway in mammalian cells. In addition, VopA, like YopJ, utilizes an evolutionary conserved mechanism for inhibition of signaling which is demonstrated by VopA's ability to inhibit MAPK signaling in *Saccharomyces cerevisiae*. I have shown that VopA is an acetyltransferase targets the MKK within the MAPK cascade revealing an activity similar to YopJ's. Through mass spectrometric analysis, I found that VopA modifies MKK on four different residues. Three of the residues, S207, K210, and T211, that are located in the activation loop, are the same residues modified by YopJ. The fourth residue, K172, is only modified by VopA and is a conserved lysine in the catalytic loop of MKKs that is required for ATP binding. I have shown that VopA's modification of this residue disrupts ATP binding and allows for the inhibition of an activated kinase.

Table of Contents

Prior Publications

Trosky, JE, Mukherjee, S, Burdette, DL, Roberts, M, McCarter, L, Siegel, RM, and Orth, K. Inhibition of MAPK Signaling Pathways by VopA from *Vibrio parahaemolyticus*. 2003. Journal of Biological Chemistry, 279(50). 51953-51957.

Liverman, ADB, Cheng, H, **Trosky, JE**, Leung, DW, Yarbrough, M, Burdette, DL, Rosen, MK and Orth, K. Direct Assembly of Actin by the *Vibrio* Type III Effector VopL. *Proceedings of the National Academy of Science.* In press.

Trosky, JE, Li, Y, Mukherjee, S, Keitany, G, Ball, H, and Orth, K. VopA Inhibits ATP binding by Acetylating the Catalytic Loop of MKKs. *Journal of Biological Chemistry.* In press.

Trosky, JE and Orth, K. *Yersinia*Yops. Cellular Microbiology. Review Submitted

List of Figures

List of Tables

List of Abbreviations

V. parahaemolyticus	*Vibrio Parahaemolyticus*
VopA	*Vibrio* outer protein A
YopJ	*Yersinia* outer protein J
TTSS	Type III Secretion System
MAPK	Mitogen Activated Protein Kinase
MKKK	MAP Kinase Kinase Kinase
MKK	MAP Kinase Kinase
ERK	Extracellular Regulated Kinase
pErk	Phosphorylated ERK
Jnk	Jun N-terminal Kinase
pJnk	Phosphorylated Jnk
NFκB	Nuclear Factor Kappa B
IKK	IκB Kinase Kinase
IκB	Inhibitor of B
TNFα	Tumor Necrosis Factor α
EGF	Epidermal Growth Factor
TDH	Thermostable Direct Hemolysin
TRH	TDH-related Hemolysin
GST	Glutathione-S-Transferase
TAP	Tandem Affinity Purification
Acetyl-CoA	Acetyl-Coenzyme A
HOG	High Osmolarity Growth
HA	Hemagglutinin
PCR	Polymerase Chain Reaction
SEK	Stress Activated Protein Kinase Kinase

TRAF	TNF receptor-associated factor
PBS2	Polymyxin B Sensitivity
Glu	Glucose
Gal	Galactose
Sorb	Sorbitol
ATP	Adenosine Triphosphate
ADP	Adenosine Diphosphate
MANT	N-methylanthraniloyl
IPTG	Isopropyl-D-thiogalactopyranoside

Chapter One

Introduction

Vibrio parahaemolyticus (*V. parahaemolyticus*) was originally discovered in Japan in 1950 as the causative agent of an epidemic of severe/fatal gastroenteritis. It has since been recognized as the causal agent of gastroenteritis throughout much of the world with the emergence of pandemic strains. Little was known about the pathogenesis of this organism except that the ability to cause disease was correlated with the presence of a toxin called Thermostable direct hemolysin (TDH) (2).

In 2003, Makino et al published the genome sequence of the clinical *V. parahaemolyticus.* strain, RimD (3). The sequence revealed that in addition to the TDH there were two type III secretion systems (TTSSs) present in the genome. One system located on chromosome I is highly homologous to the *Yersinia spp.* TTSS except for a cluster of open reading frames (ORFs) of unknown function. These have been proposed to be the secreted effectors or chaperones (4). This system is found in both environmental and clinical strains possibly indicating a role in survival within the environment. The second system is located on chromosome II within a pathogenicity island that also encodes the genes for TDH. Another interesting feature of this island is the presence of a gene that encodes a homologue of the *Yersinia spp.* Type III effector YopJ called VopA.

The overall focus of this thesis is the molecular characterization VopA. I have shown that this protein inhibits MAP kinase signaling in mammalian cells via an evolutionary conserved mechanism. I was able to show that VopA functions as an acetyltransferase targeting the MAP kinase kinase (MKK) within the signaling pathway. VopA is able to inhibit activated kinases by acetylating a critical lysine in the catalytic loop disrupting ATP binding.

Chapter Two

Literature Review

Discovery of *Vibrio parahaemolyticus*

October 20th and 21st, 1950 272 people were struck with acute gastroenteritis in the southern suburbs of Osaka, Japan. Of the 272 patients, 20 people died from illness. Symptoms of the outbreak included acute abdominal pain, vomiting and watery diarrhea and in some cases bloody diarrhea. The source of the outbreak was believed to be shirasu, a small, half-dried sardine. To identify the responsible agent, Fujino and colleagues utilized a guinea pig model to test filtered homogenates of shirasu to rule out possible chemical poisoning. The guinea pigs developed peritonitis. The homogenates were then inoculated onto culture medias in both aerobic and anaerobic conditions to identify the presence of individual types of bacteria. The group isolated *Lactobacillus* and *Staphylococcus* along with an unidentified gram-negative rod that formed white, opaque colonies.

Upon further investigation it was observed that these opaque colonies consisted of two types of bacteria. Attempts to separahaemolyticuste these two organisms by streaking on plates were unsuccessful; so an attempt to separahaemolyticuste these two bacteria by animal passage was made. A suspension of the two bacteria was inoculated intraperitoneally into mice. After

several hours symptoms of disease appeared and samples of ascitic fluid were taken. After incubation on blood agar two different types of bacteria were identified: a slender nonhemolytic rod, *Proteus morganii,* which produced acid and gas in glucose and did not hydrolyze gelatin, and a fat rod demonstrating bipolar staining that produced acid but not gas from glucose, liquefied gelatin and was pathogenic to mice. They were also able to isolate this organism from the stool samples of affected patients. Fujino and colleagues named this organism *Pasteurella parahaemolyticushaemolytica.* Subsequent studies of this organism led to it being renamed *Vibrio parahaemolyticus* (*V. parahaemolyticus.*) (2). Since its discovery in the 1950s *V. parahaemolyticus* has since been found to be one of the leading causes of gastroenteritis associated with the consumption of seafood throughout the world (5).

The Many Lifestyles of *Vibrio parahaemolyticus*

Since the initial outbreak of *V. parahaemolyticus.* this pathogen has been found to be a ubiquitous marine organism found in a wide variety of environmental niches. The different niches are indicative of the different lifestyles of *V. parahaemolyticus.* including a free-swimming state, within microbial communities either attached to shellfish or the bottoms of boats or other surfaces, or as a pathogen in a host organism. For each niche *V. parahaemolyticus.* expresses a set of characteristics that are necessary for survival within each environment.

The Swimmer Cell

The free-living form of *V. parahaemolyticus.,* or the swimmer cell, is characterized by the presence of a single polar flagellum (Fig. 1). The polar flagellum is powered by the sodium motive force. This is advantageous in seawater given that the average pH is 8.0, which means sodium ions are more readily available than protons. These motors are very fast with average speeds of 60μm per second. The structure of the flagellum is complex as it is constructed of six different polar flagellin proteins. The flagellum is sheathed and plays a key role in the initial attachment to surfaces. The exact role of the sheath is not well understood, but it could play a role in attachment to a specific surface depending on the surface proteins present in the flagellar sheath (6).

In addition to its role in motility the polar flagellum appears to play a role in the switch from the swimmer to the swarmer cell. The function of the polar flagellum is linked to expression of the lateral flagellar system. Although, the polar flagellum is constitutively expressed, conditions that perturb the function of the polar flagellum can lead to the expression of the lateral flagellar system (7). In this way the polar flagellum system serves as a mechanosensor signaling to the cell as to what kind of environment it is in and enabling the cell to induce the necessary changes.

The Swarmer Cell

The swarmer cell type is typically found when *V. parahaemolyticus* grows on solid media or in viscous environments. This type is characterized by two major morphological shifts from the swimmer cell (Fig. 2). First the cell elongates from lengths of 2μm up to lengths of 30μm as septation ceases. The other shift in morphology stems from the expression of the lateral flagellar system. The lateral flagellar system is characterized by the enumeration of numerous peritrichously arranged flagella around the cell. These flagella are simpler than the polar flagellum because they are not sheathed and are synthesized from a single flagellin protein. The flagella are also very sensitive to shearing from mechanical forces, and detached flagellar aggregates are easy to isolate from culture media and view under a light microscope. In addition to the perturbation of the polar flagellum the lateral flagellar system can also be induced under iron limiting conditions (6). It is unknown if the lateral flagellar system plays a role during infection but given the viscous environment and iron limiting conditions within the host this system could play a role in invasion and establishment of infection.

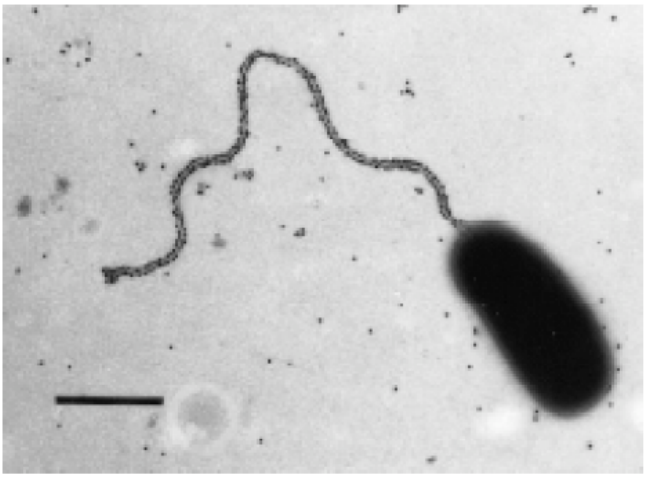

Figure 1: Electron Micrograph of a Swimmer Cell. Electron micrograph of a swimmer cell reacted with rabbit antiserum prepared against whole cells and detected by 15nm protein A-bound colloidal gold particles. Bar indicates approximately 1 mm. (6)

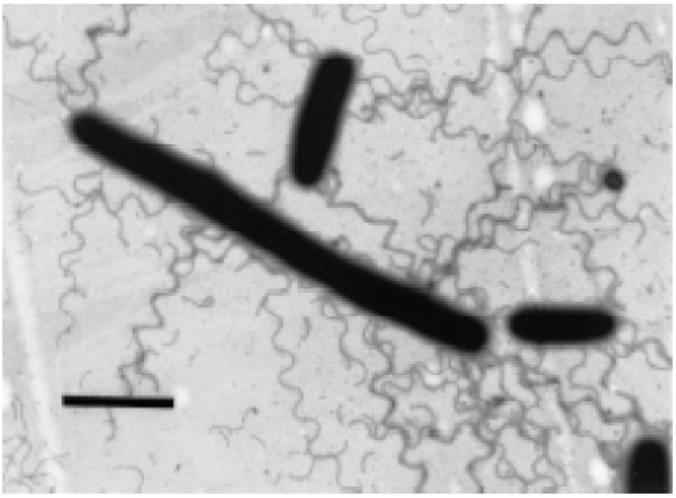

Figure 2: Electron Micrograph of a Constitutive Swarmer Cell. Grown in liquid and negatively-stained with 0.5 % phosphotungstic acid. Bar indicates approximately 3 mm. (6)

Opaque versus Translucent

In addition to the variations in flagellar systems, *V. parahaemolyticus.* also exhibits variations in colony morphology, growing as opaque or translucent colonies (Fig. 3). The description stems from the transmission of light through the colonies. Opaque cells aggregate in certain types of liquid, possess a thick capsular material that stains with ruthenium-red, have a specific set of outer membrane proteins and swarm very poorly. In contrast, translucent cells lack a capsule and are very good swarmers. It is believed that these differences between the cell types are what give the colonies their differential morphology (4).

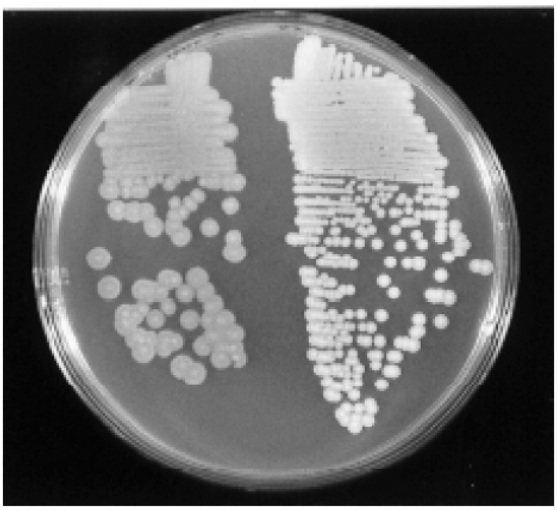

Figure 3: Opaque and Translucent Colonies. Opaque colonies are shown on the right and translucent colonies are shown on the left. (4)

The switch from opaque to translucent is controlled by a homolog of the global regulator LuxR called OpaR. In *Vibrio harveyi* LuxR is a regulator of luminescence, and homology between LuxR and OpaR suggests that OpaR might also interact with autoinducers (6). This would indicate that the switch between translucence and opacity is controlled by cell density. OpaR is only expressed when cells are opaque and its expression is repressed in translucent cells. Regulation of OpaR

expression is not very well characterized but its regulation is speculated to be controlled by environmental and or intracellular cues (6).

Pathogenesis of *Vibrio parahaemolyticus*

V. parahaemolyticus is a leading cause of gastroenteritis associated with the consumption of seafood that is either handled improperly or consumed raw. Its presence in coastal waters typically follows a seasonal cycle with high counts in the summer and early fall when waters are warm and counts falling in late fall and winter as waters cool (1). Symptoms typically associated with disease include diarrhea with abdominal cramping, nausea, vomiting and fever. The diarrhea is sometimes bloody and watery; this effect is referred to as "meat washed" due to the coloration. Illness is usually self-limiting and rarely requires treatment in immunocompetent patients (5,8). In addition to gastroenteritis, *V. parahaemolyticus* infection can also result in wound infections and septicemia. Septicemia and wound infections are rare but are usually associated with individuals with underlying liver disease, alcoholism or diabetes (5).

Thermostable Direct Hemolysin

All *V. parahaemolyticus.* strains isolated from patients express the thermostable direct hemolysin (TDH) or the TDH-related hemolysin (TRH). TDH causes β-hemolysis on a special type of agar known as Wagatsuma agar; this is known as the Kanagawa phenomenon (9). The levels of β-hemolysis can vary from strain to strain. TDH is a hemolysin that induces lysis in erythrocytes. In

addition to its hemolytic activity, TDH has also been implicated in affecting the calcium homeostasis and modulating cytoskeletal organization in cultured intestinal cells (10). The mechanism for how TDH elicits its function remains elusive though freeze fracture analysis of membranes treated with TDH show the formation of pore-like structures in the membrane.

TDH is named for its properties. It is inactivated by heating at 60°C but is stable when heated to 100°C. This is known as the Arrhenius effect and was a puzzling characteristic of this protein until microscopic analysis of the protein heated to 60°C revealed that it forms amyloid fibrils (11). Amyloid fibrils are formed by a number of proteins some of which are associated with disease. These fibrils are rich in β-sheets and highly stable. It is unknown whether the formation of amyloid fibrils contributes to the toxicity of TDH, However the hemolytic activity of TDH is suppressed by the addition of the dye Congo red which is known to be sensitive to amyloid fibrils. Also the fibrils were stabilized when associated with lipid membranes suggesting that there could possible be a role for these fibrils in toxicity (11).

Expression of TDH is known to be controlled by *toxRS* homologues. The *toxRS* system is a set of transmembrane regulatory proteins that regulate the expression of the cholera toxin in *Vibrio cholerae*. The predicted *V. parahaemolyticus.* ToxRS proteins show a similar domain structure to the *Vibrio cholerae* (*V. cholerae*) ToxRS proteins indicating that they might work in a

similar manner (12). *V. parahaemolyticus.* strains differ in their ability to cause β-hemolysis on Wagatsuma agar. The differences are related to the regulation of expression of TDH. Although there is little variation in the *toxRS* genes, promoter analysis reveals changes in the promoter sequence leading to differences in the promoter strength. Therefore variations in the ability to induce hemolysis are reflected in a simple relationship between the amount of TDH produced and the extent of β-hemolysis (9).

Emergence of Pandemic Strains

Beginning in 1996 there was an increase in the number of cases of *V. parahaemolyticus* related gastroenteritis. One serotype was consistently isolated from these patients, the O3:K6 serotype. An analysis of an outbreak in Calcutta indicated that the O3:K6 serotype accounted for 50-80% of the patients in this outbreak. The O3:K6 serotype had been found in Japan between 1983 and 1988 but all were TDH negative (13). It has been speculated that perhaps the virulent O3:K6 strains might have originated from these strains having acquired the *tdh* genes from the environment (13). An increase in *V. parahaemolyticus.* infections caused by the O3:K6 serotype were also observed in other parts of the world, including the US. The increase *V. parahaemolyticus* infections peaked in the US between 1997 and 1998 (8). These were also El Niño years so the increase in infections could also be attributed to the warmer waters caused by this weather system (8). The O3:K6 serotype has spread globally and has been isolated in

Europe, Africa, Asia, South America and North America (Fig. 4). The widespread nature of the O3:K6 serotype led to its description as a pandemic, but it has not demonstrated a significant increase in the number of people infected. In contrast to other pandemics such as the *V. cholerae* el Tor biotype (8), as whether or not the O3:K6 serotype is truly a pandemic strain is still debated.

Type III Secretion Systems

Type III secretion systems (TTSSs) are a common virulence factor among gram-negative bacteria. The secretion apparahaemolyticustus is a large needle-like apparahaemolyticustus that spans the inner and the outer membrane of the bacteria. The needle serves as a conduit delivering effector proteins directly into the host cell cytosol (14). Although the structure of the type III secretion apparahaemolyticustus remains essentially the same from one organism to another each organism regulates the system differently and encodes a unique set of effectors that is most beneficial to the pathogen (14). For example, *Yersinia spp.* utilize an array of six effectors to prevent uptake and inhibit the innate immune response thereby allowing for establishment of an extracellular infection (15). In contrast, *Salmonella* encodes two TTSSs to induce its uptake into cells and to maintain itself within the host cells (16). When the *V. parahaemolyticus.* genome was sequenced, it revealed the presence of two TTSSs (3). Both TTSSs were located in pathogenicity islands, one on the larger chromosome I (TSS1) and the other on the smaller chromosome II (TTSS2). Subsequent analysis revealed that

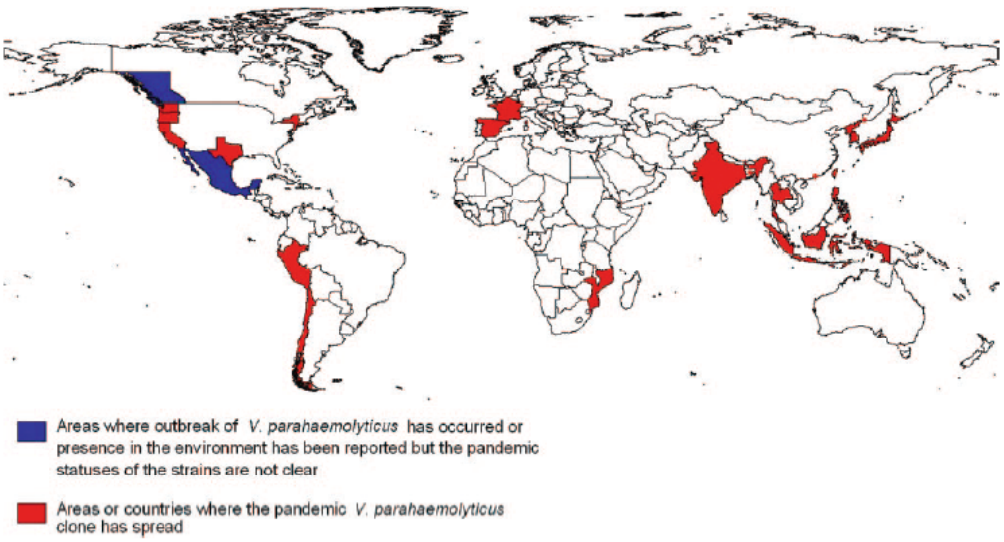

Figure 4: Map showing Dissemination of the O3:K6 Serotype. (8)

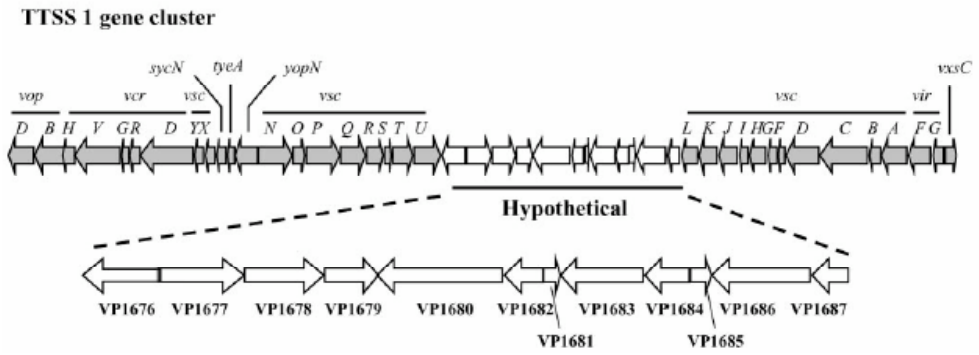

Figure 5: *V. parahaemolyticus.* TTSS1 gene cluster located on chromosome 1. The TTSS apparahaemolyticustus genes are similar to those of *Yersinia* spp. except for the presence of a hypothetical region between them. This includes 12 hypothetical genes, which were all identified as encoding hypothetical proteins (17).

the TTSS1 was found in all strains including environmental whereas the TTSS2 was found exclusively in clinical isolates. This observation leads to speculation as to the uses of each of these systems. Could TTSS1 be useful within the environment as a defense against predators or in the establishment of symbiotic relationship? Is TTSS2 required for survival during incidental infections and does it work in conjunction with TTSS1 during infection?

Chromosome I Pathogenicity Island

The pathogenicity island located on chromosome I encodes a type III secretion system that is highly homologous to the TTSS found in *Yersinia spp.* The major differences between the two loci is that the *V. parahaemolyticus.* locus is in the reverse order of the *Yersinia spp.* locus and there is a set of twelve open reading frames (ORFs) that are predicted to encode hypothetical proteins. These open reading frames (ORFs), VP1680 and VP1682, VP1683 and VP1684, and VP1686 and VP1687, are predicted by bioinformatics to encode effector/chaperone pairs (4). VP1680, VP1683, and VP1686 were also identified as secreted effectors along with VPA450 using 2d gel analysis of culture supernatants from a wild-type strain and a TTSS1 knockout strain (17). Both VP1680 and VP1686 have been found to induce cytotoxicity in cell culture. In infection models, the TTSS1 is required for cytotoxicity but does not appear to affect enterotoxicity in a rabbit ileal loop model (18). The lack of an effect in the rabbit ileal loop model by TTSS1 may be for two reasons: first, the system does

not play a role during infection and/or second, it requires the TTSS2 to act first and then the TTSS1 is engaged. To address these issues a more thorough understanding of the effects and regulation of both of these systems is required.

Chromosome II Pathogenicity Island

The chromosome II pathogenicity island exhibits many of the characteristics of a "classic" pathogenicity island. The island has insertion elements located at both ends and the G+C content is lower then the rest of the genome (39.8% compared to 45.4% for the rest of the genome) suggesting that these genes were acquired through a recent lateral transfer (Fig. 6) (19). This island also encodes the *tdh* genes and the *toxRS* genes; genes already known to be involved in virulence. In addition this island also contains the necessary structural genes for a second TTSS. There are also other genes located in the island that are candidates for virulence factors including VPA1321, a homologue of the *E.coli* protein cytotoxic necrotizing factor-1 is a deamidase affecting Rho, Rac and CDC42 function (20); VPA1327, a homologue of the *Pseudomonas* effector ExoT, an ADP-ribosyltransferase targeting signaling at the focal adhesions (21); VPA1370 or VopL, which induces actin assembly both *in vitro* and *in vivo* (Liverman et al, in press); and VPA1346 or VopA, a homologue of the *Yersinia spp.* effector YopJ which inhibits MAPK and NFκB signaling (Fig.6) (22). VPA1327, or VopT was recently demonstrated to function as an ADP-ribosyltransferase targeting Ras (23). The TTSS2 has been shown to be required for cytotoxicity in a rabbit ileal

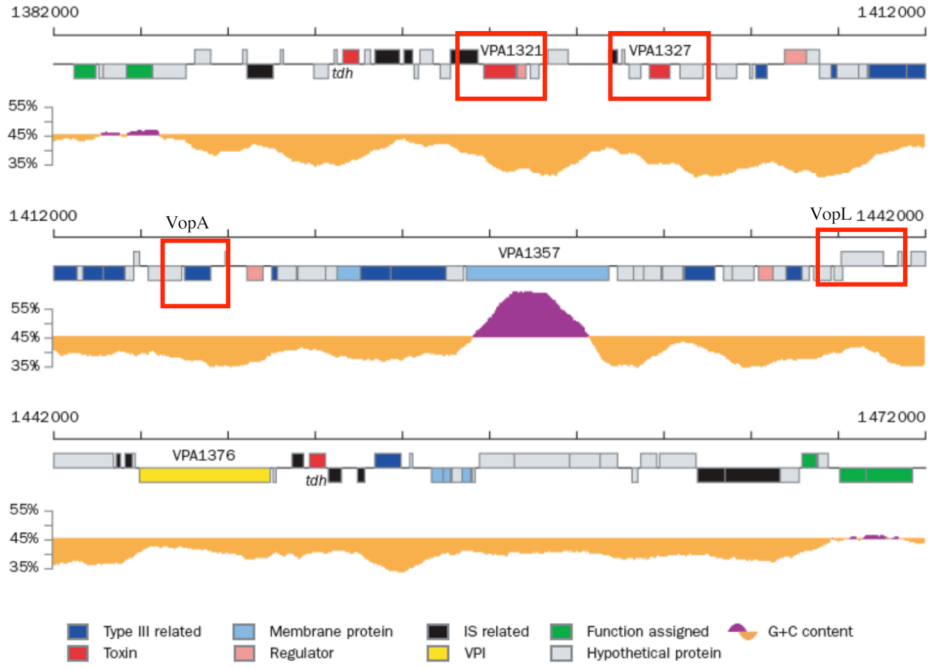

Figure 6: Representation of *V parahaemolyticus* Pathogenicity Island. Top line shows the position on chromosome 2 in bp from the replication origin. Second line represents genes as blocks; those found on the plus strand are shown above the line, and those on the opposite strand are shown below. The third line shows the percentage G+C content; higher and lower content than the average are depicted by purple and yellow, respectively. Type III related=proteins related to the type III secretion system; toxin=genes encoding a toxin or an enzyme that is reportedly involved in pathogenesis of other bacteria; regulator=transcriptional regulator; IS related=genes related to insertion sequences or transposons; VPI=a homologue of a gene present in VPI; function assigned=genes with known function. Red boxes highlight potential virulence factors. VPA1321 and VPA1327 encode the homologue of *Escherichia coli* cytotoxic necrotizing factor and *Pseudomonas* exoenzyme T, respectively. VopA is a homologue of the *Yersinia spp.* effector YopJ, and VopL has homology to actin binding proteins. (3)

loop model of infection. This data along with the presence of this system in all clinical isolates implies that this system is required for virulence in humans.

YopJ Family of Proteins

The YopJ family of proteins is a family of type III secreted effectors known to modulate host signaling pathways upon injection. YopJ proteins are found in a wide variety of bacteria including animal pathogens, plant pathogens and plant symbionts. This family is characterized by their effects on host signaling pathways and the presence of a conserved catalytic triad with catalytic activity required for function. The founding member of this family YopJ is a type III effector found in *Yersinia spp.* YopJ has been shown to inhibit both MAPK and NFκB signaling (Figs. 7 and 8, respectively) in cells at the level of MKK and IKKβ, respectively (22,24). This inhibition was found to be mediated through an evolutionarily conserved mechanism due to its ability to inhibit MAPK signaling at the same level in budding yeast (Fig. 9) (25).

The mechanism of YopJ's function remained elusive. The first hints of its mechanism were found in secondary structure predictions. These predictions aligned YopJ with the known secondary structure of adenovirus protease (AVP); this alignment aligned the catalytic triad of AVP with an almost identical catalytic triad in YopJ (24). An observation by Li and Hochstrasser noted that AVP's secondary structure was similar to the yeast ubiquitin-like protein protease (ULP-1) (26). Due to the alignment of YopJ and AVP it was proposed that YopJ

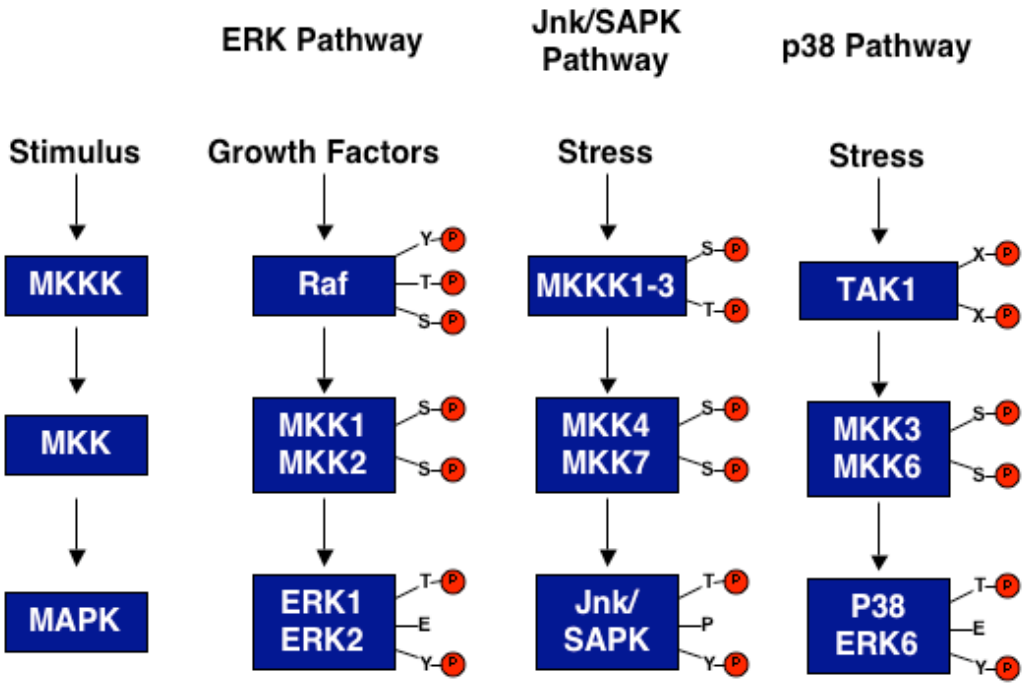

Figure 7: Schematic Representation of Mammalian MAPK Pathways.

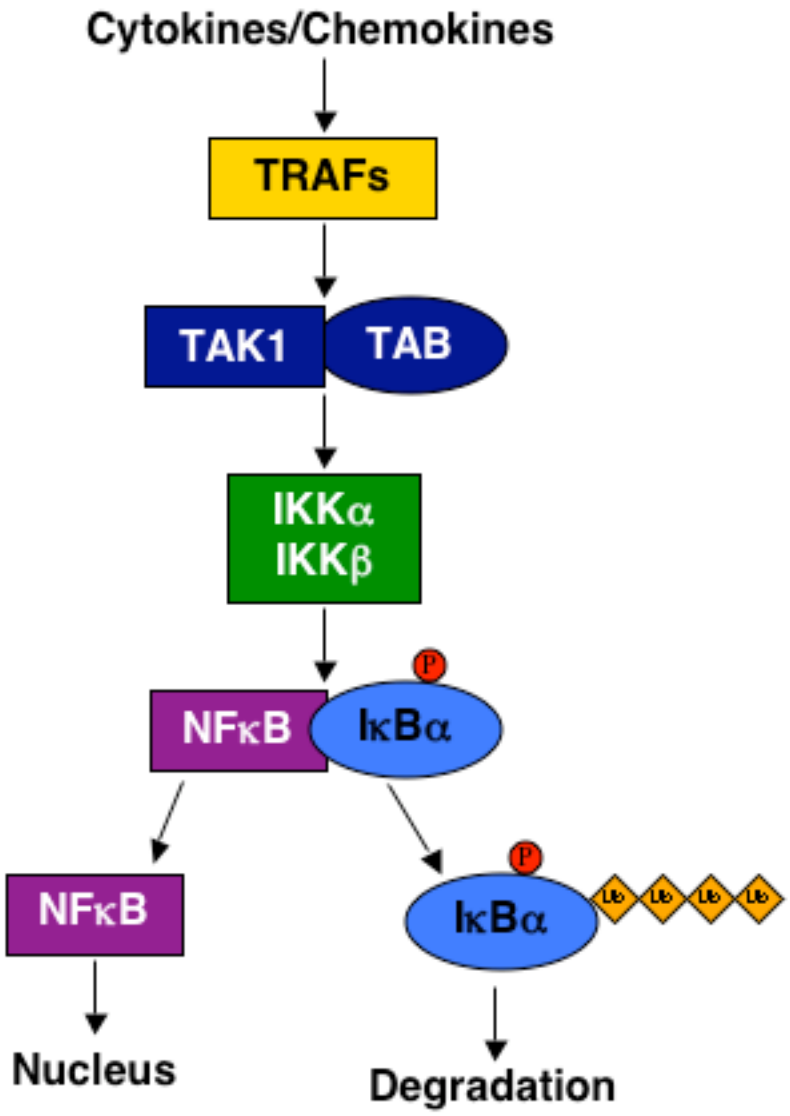

Figure 8: Schematic Representation of the NFκB Pathway.

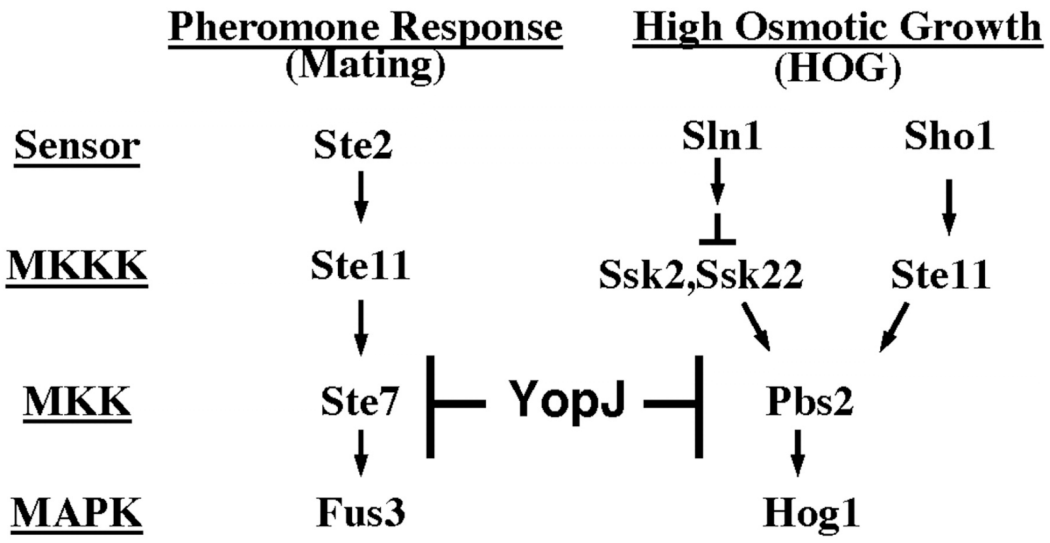

Figure 7: Schematic representation of the Mating and HOG MAPK pathways. The third branch of the osmo-sensing pathway and other components of these pathways are omitted for clarity. YopJ is proposed to act at the level of the MAP kinase kinase (*MKK*). *MKKK*, MKK kinase (25).

functions as a deSUMOylating enzyme. It was observed that upon transfection of YopJ there was what appeared to be a decrease in the total amount of SUMOylated proteins. However these results were unable to be confirmed in a variety of *in vitro* and *in vivo* assays (28).

Studies had shown that YopJ binds to and affects MKKs and IKKβ. An *in vitro* signaling assay was developed that showed YopJ's ability to inhibit these pathways *in vitro.* Through a combination of coexpression of GST-YopJ and His-MKK6 and mass spectrometric analysis, Mukherjee et al (1) were able to demonstrate that YopJ functions as an acetyltransferase. They found that YopJ acetylates the critical serine and threonine in the activation loop, thereby, utilizing a simple mechanism of acetylation blocks phosphorylation. A recent study on the YopJ homologue AvrBst from the plant pathogen *Xanthomonas campestris pv. vesicatoria* also support this mechanism. In this study the activity of AvrBst was found to be suppressed by expression of a conserved carboxylesterase named Suppressor of AvrBst –Elicited Resistance 1 (SOBER1). SOBER1 was shown to deacylate a panel of chromogenic substrates in *in vitro* assays. If AvrBst functions as an acetyltransferase than the resistance factor SOBER1 can function to counteract its effect by deacylating AvrBst target proteins. VopA, the YopJ homologue in *V. parahaemolyticus.,* shares about 55% sequence identity with YopJ. Given the similarity of the two effectors and the known functions of other YopJ-like effectors, it was speculated that VopA also affects signaling pathways by a similar mechanism.

Chapter Three

Materials and Methods

Chapter 4

Cloning of Effectors—VopA was amplified by PCR from *V. parahaemolyticus* genomic DNA with a 5 -HindIII primer and a 3 -FLAG-stop-ApaI primer and cloned into the mammalian expression vector pSFFV. The VopA alanine mutant was generated by site-directed mutagenesis using the Stratagene QuikChange mutagenesis kit. VopA and VopA-C167A were amplified by PCR using pSFFV VopA or pSFFV VopA-C167A as template with 5 -EcoRI and 3 -FLAG-stop-XhoI primers and cloned into the yeast expression vector pRS413 under control of the GAL promoter. All constructs were confirmed by DNA sequencing.

MAPK Assays—293T cells were transfected with or without a MAPK (HA-ERK; 100 ng) in the presence or absence of YopJ-like effector plasmids (100 ng). And after 48 h of growth, cells were starved for 3 h followed by treatment or no treatment with a stimulus (epidermal growth factor, 50 ng/ml). Cells lysates were analyzed by immunoblot analysis with rabbit anti-phospho-ERK antibody (Cell Signaling Technology, Inc.) and mouse anti-HA antibody (Babco). YopJ-like effectors were detected using mouse anti-FLAG antibody (Sigma).

NFκB Assays—293T and HeLa cells were transfected with or without FLAG-IκB (1 μg) in the presence or absence of YopJ-like effector plasmids (50 ng). After

36h of growth, 293T cells were treated with TNFα (50 ng/ml) for 30 min, and HeLa cells were treated with interleukin-1β (10 ng/ml) for 15 min. Cell lysates were analyzed by immunoblot analysis with rabbit anti-phospho-IκB antibody (Cell Signaling Technology, Inc) and mouse anti-FLAG antibody (Sigma).

Death Assays—Jurkat cells were transiently transfected using a BTX ECM electroporator (260 V, 1050 microfarads, 720 ohms) with 10 μg of each plasmid and 2 μg of pMEM-YFP membrane-bound yellow fluorescent protein (Clontech) as a transfection marker. Twenty-four hours later, cells were left untreated or treated with 100 ng/ml human TNFα for ~18 h. Death was assessed by flow cytometric analysis of annexin V-activated protein C binding and propidium iodide. Live cell percentages were calculated as the percentage of yellow fluorescent protein positive cells that were annexin V and propidium iodide negative. Specific cell death was calculated using the formula 100 × (1−TNFα treated/untreated) for the live cell percentages in each condition.

Yeast Growth and MAPK Assays—Yeast cells expressing the indicated empty vector or the YopJ-like effector plasmids were assayed for growth by plating on glucose media, galactose media, or galactose media containing 1 M sorbitol. For growth curves, overnight cultures grown in glucose were diluted back to an OD of 0.1 in 20 ml of indicated media, and the absorbance was measured at 600 nm. For MAPK assays, yeast cells containing either an empty vector or YopJ, YopJ C/A, VopA, or VopA C/A vectors under control of the galactose promoter were grown

to mid-log phase in glucose media and then shifted to galactose media to induce protein expression for 3 h. Cells were then induced with either 0.7 M sorbitol for 2.5 min or 12 mM caffeine for 1 h. Protein extract from these cells were isolated as described in Yoon *et al.* (25) and analyzed by immunoblotting with anti-phospho-p38 antibody (Cell Signaling Technology, Inc.) or anti-phospho-p44/42 MAPK antibody (Cell Signaling Technology, Inc.), anti-FLAG antibody, and anti-porin antibody (loading control).

Accession Numbers—The GenBankTM accession number for YopJ is AY606230 and for VopA is AY597337.

Chapter 5

Cloning— pSSFV VopA-Flag and pSFFV VopA-C167A constructs were generated as described for chapter 4. For bacterial overexpression, VopA and VopA-C167A were amplified by PCR using pSFFV VopA or pSFFV VopA-C167A as template with 5`-EcoRI and 3`-stop-XhoI primers and cloned into pGEX-TEV (a kind gift of Y.M.Chook). This places a GST tag on the N-terminus of VopA with both thrombin and TEV cleavage sites in the linker. For the yeast two-hybrid construct, pLexAde-VopA, VopA was amplified by PCR using pSFFV-VopA as template with 5`-EcoRI VopA and 3'-BamHI VopA primers with no start codon and cloned into pLexAde. This makes a fusion protein with the DNA binding protein from *E.coli* LexA on the N-terminus and VopA for TAP-tag purification VopA was amplified by PCR using pSFFV-VopA as

template with 5`- BamHI VopA and 3'-NcoI VopA primers with no stop codon. The TAP-tag was amplified from pBS1479 with 5`- NcoI TAP with no start codons and 3'- TAP XhoI primers, a yeast vector for genomic tagging (a kind gift of A. Shilatifard). The TAP-tag and VopA PCR fragments were cut and co-ligated into the yeast expression vector pRS413 under control of the GAL promoter with the TAP-tag at the C-terminus of VopA.

Yeast Strains for Two-Hybrid Screen—Two yeast strains were utilized in the two hybrid screens the bait strain, L40, and the mating strain AMR70 (29). The genotype of L40 is *MATa his3 trp1 leu2-3 ade2 LYS2::(lexAop)$_4$-HIS3 URA3::(lexAop)$_8$-lacZ GAL4.* This strain contains two integrated reporters, a *his3* reporter under the control of four LexA operators and secondly a LacZ reporter under the control of eight LexA controllers. The genotype of Amr70 is *MATα his3 lys2 trp1 leu2 ade2 URA3::(lexAop)$_8$-lacZ GAL4.* This strain is commonly used for mating with L40 to check positive identified in two-hybrid screens. pLexAde-VopA was transformed into the bait strain. To test for autoactivation of VopA in this system, the L40 strain with pLexAde-VopA was transformed with the library vector, pVP16, by the lithium acetate protocol and streaked onto YC-WHULK media to test for activation of the *his3* gene.

Yeast Media for Two-Hybrid Screen—Yeast strains were routinely cultured in the rich media YPAD composed of 10g yeast extract, 20g bacto-peptone, 0.1g adenine, 2% (w/v) glucose (20% stock added after autoclaving), 20g agar as

needed per liter. YPA is YPAD without glucose. For plasmid selection yeast strains were cultured in synthetic complete media composed of 1.2g yeast nitrogen base minus amino acids and ammonium sulfate (Difco), 5g of ammonium sulfate, 10g of succinic acid, 6g of sodium hydroxide, 0.75g of WHULK minus amino acid and pyrimidine mix, 2% (w/v) glucose (20% stock added after autoclaving), and essential amino acids which could include a mix of the following: 0.05g histidine, or 0.1g of tryptophan, uracil, leucine, or lysine. Omission of tryptophan selects for the bait plasmid (pLexAde), omission of leucine selects for the library plasmid, omission of uracil selects for the lacZ integrated reporter, omission of lysine selects for the *his3* integrated reporter, and omission of histidine selects for interactions between the bait protein and the library.

Yeast Two-Hybrid Library Transformation—To test for binding partners of VopA the bait strain was transformed via a long transformation protocol with a short HeLa library in pVP16 (29). For the long transformation the bait strain was inoculated into YCD-HU (5mL) and grown overnight at 30°C. The culture was then expanded by inoculation into YCD-HU (100 mL) and grown overnight at 30°C to an OD_{600} of 4 or less. This culture was then diluted to an OD_{600} of 0.3 into 500mL of prewarmed YPAD and grown at 30°C for 4 hrs. Cells were then pelleted and washed with 250mL of 1x lithium acetate, 0.5xTE. Then resuspend cells in 10mL of 1x lithium acetate, 0.5xTE in a large flask. Then add a DNA

mixture (1mL) containing 500μg of HeLa cDNA library plasmid and 10mg of denatured salmon sperm DNA to the cell suspension. Add 70mL of 1x lithium acetate, 40% polyethylene glycol 3350 (PEG)(Sigma) and 1xTE and incubate cells at 30°C for 30 min. After 30 min add 8.8mL of dimethyl sulfoxide (DMSO) (Sigma) to the cells and incubate at 42°C 6min swirling the flask periodically. The cells were diluted in 200mL of YPA and cooled to room temperature on ice. The cells were pelleted and washed with 250 mL of YPA. The cells were resuspended in 500 mL of YPAD and grown at 30°C for one hour. To determine the primary transformation efficiency, 1 ml of cells were removed, pelleted and resuspended in 1mL of YC-WUL. Dilutions (10μL and 1μL) were plated in triplicate on YC-WUL plates and incubated at 30°C for 2-3 days or when the colonies could be counted. The remaining cells were pelleted, washed in 250mL of YC-WUL, and then resuspended in 500mL of YC-WUL. The culture was grown at 30°C overnight to allow for *his3* activation. The cells were pelleted, and washed twice in YCD-WHULK. Cells were resuspended in 20ml of YCD-WHULK. Dilutions (10μL and 1μL) were plated on YCD-WUL to determine the number of doublings. To select for positives aliquots of 5, 10, 25, and 50μL were plated onto 10 plates each of YCD-WHULK. Plates were incubated at 30°C until colonies appeared (2-3 days). To determine the number of plates to screen the number of doublings of the primary transformation to the plated library was determined. Then calculated the amount of the library plating equivalent to three

times the complexity of the primary transformation ((1/number of doubling)×amt of suspension×3).

β-Galactosidase Filter Assay—To test for β-Galactosidase activity, a grid of his+ colonies were overlayed with a dry nitrocellulose filter (BA-S85, 82mm, Schleicher and Schuell). Colonies were transferred to the nitrocellulose by gently pressing on the filter. The filter was lifted and submerged yeast side up on an aluminum boat in liquid nitrogen to lyse cells. 1.5mL of Z buffer (60mM Na_2HPO_4, 40mM NaH_2PO_4, 10mM KCl, 1mM $MgSO_4$ (pH7.0)) and 100μL of X-gal (50mg/mL in N,N-dimethylformamide) were placed in the top of Petri dish. Then a filter paper circle was placed in the dish followed by the nitrocellulose colony side up. This was then incubated at 30°C until color appeared, usually about 30 minutes.

Segregation of Library Plasmid—To segregate the library plasmid from the bait plasmid positive from the two-hybrid screen were streaked for individual colonies onto YCD-L plates with low adenine (10mg/L). Under these conditions, colonies that have lost the bait plasmid will turn pink due to the loss of the *ade2* gene encoded by the bait plasmid and the resulting block in the adenine biosynthetic pathway. Pink colonies were passaged multiple times on YCD-L with low adenine. To confirm loss of the bait plasmid, pink colonies were patched onto YCD-WUL to check for growth. Those that did not grow were then used in mating assays.

Mating Assay—Overnight cultures of library strains and of the mating strains AMR70 with empty bait plasmid to test for autoactivation, bait plasmid expressing Lamin to test specificity and pLexAde VopA were grown at 30°C. Matings were spotted in grids on YPAD with 1μL of the library strain and then overlayed with 1μL of the mating strain. Matings were grown overnight at 30°C. Colonies were transferred to sterile velvets and replica plated onto YCD-LW to select for diploids. Plates were incubated at 30°C for 2 days. Diploids were then tested using the β-galactosidase assay.

GST Pulldown from HeLa Lysate— GST VopA WT and GST constructs were expressed in *Escherichia coli* BL21-DE3 cells and purified by GST affinity chromatography. In brief, cells were grown to *A*600 0.6–0.8 in 2x yeast extract and tryptone medium and then induced with 400 μM isopropyl-D-thiogalactopyranoside (Roche Applied Science) (IPTG) for 4 h at 25°C. The cells were lysed in phosphate-buffered saline (pH 8), 1% (v/v) Triton X-100 (Fisher), 0.1% (v/v) 2-mercaptoethanol (Bio-Rad), and 1 mM phenylmethylsulfonyl fluoride (Sigma) (PBS-T) using a cell disrupter (EmulsiFlex-C5, Avestin Inc.). The lysates were incubated with glutathione agarose beads at 4°C. Beads were washed 3x in PBS-T for ten minutes each. Bound protein was purified fresh for each experiment. HeLa cells were routinely cultured in DMEM supplemented with 10% heat inactivated fetal calf serum (Hyclone), penicillin/streptomycin/glutamate (Invitrogen) and sodium pyruvate (Invitrogen).

Two days before the pulldown HeLa cells from five 100mm dishes were split 1:2 (5mLcells in 12mL total) into 150mm dishes. For harvest, HeLa cells were washed in 3mL PBS per plate and trypsinized with 2mL trypsin (0.05% trypsin, Invitrogen). Cells were scraped from dishes and plates were washed with PBS-EDTA. Cells were then pelleted and washed in 1x PBS. Supernatant was removed and the cells were lysed in an equal volume of TX buffer (0.5% Triton X-100, 10mM Hepes, 10mM $MgCl_2$, 1mM $MnCl_2$ and 0.1mM EGTA). Let incubate on ice for one hour. After lysis, lysates were cleared by centrifugation at 10kxRPM for 10min at 4°C. 320µL of the cleared lysate was incubated with 100µL of the GST-VopA or GST beads on a nutator at 4°C for one hour. Beads were washed 3x with Tx-100 buffer. 5x SDS sample buffer was added to each sample (1:1). Samples were separahaemolyticusted on SDS-PAGE and gels were stained by either silver stain or coomassie blue stain. For identification of bands, samples were separahaemolyticusted by SDS-PAGE and then stained with colloidal blue (Invitrogen) as required by the protein identification lab. Gel slices were then taken to the Univ. of Texas Southwestern lab for protein identification.

TAP-Tag Purification—p413 VopA-TAP was transformed into the wild type yeast strain BY4741. Overnight cultures of this strain were diluted back to an OD_{600} 0.1 in 1.5L of YPAD and grow overnight at 30°C. The following day cells were pelleted and washed 2x in water. Cells were resuspended in 1.5L of YC-H Gal and grown at 30°C to induce VopA-TAP expression. After 3hrs cells were

pelleted and stored at -80°C. Cells were resuspended in 20mL of YEB and complete protease inhibitor tablet (Roche). Cells were lysed using a cell disruptor (Emulsiflex-C3 High Pressure Cell Homogenizer, Avestin, Inc.) at 27,000 kPa for 2 min. Lysates were ultracentrifuged in 11.5mL ultracentrifuge tubes (Sorvall, Cat. No 03987) at 33.5 kRPM at 4°C for 2 hours. Supernatant was then dialyzed from the YEB buffer to dialysis buffer, overnight which switches the lysate from a KCl buffer to a NaCl buffer with glycerol. The dialyzed lysate was then centrifuged in 11.5mL ultracentrifuge tubes at 33.5 kRPM at 4°C for 30min to remove anything that might have precipitated during dialysis. 10% Triton X-100 was added to supernatant to a final concentration of 0.1%. The supernatant was then transferred to a tube containing 300μL of IgG beads (CalBiochem) washed 2x with IPP buffer and incubated at 4°C for 3-4 hrs on a nutator. Slurry was poured into a disposable polypropylene column (Bio-Rad) and beads were washed 5x with IPP buffer and 2x with TEV cleavage buffer. The bottom of the column was closed and 200μL of TEV cleavage buffer and GST-TEV was added. The top of the column was closed and incubated on a nutator at 4°C overnight. The eluate was recovered by gravity flow and the column washed with 200μL of TEV cleavage buffer. Eluate was then passed over a GST column (100μL) 3x to remove the GST-TEV. One volume of calmodulin binding buffer and 3μL 1M

Table 1: YEB Buffer (50mL)

Final Concentration	Stock Solution	Amt of stock for 50mL
245mM KCl	1M KCl	12.25mL
3mM EDTA	0.5M EDTA	300µL
5mM EGTA•KOH	0.5M EGTA•KOH pH7.9	500µL
100mM HEPES•KOH	1M HEPES•KOH pH7.9	5mL
H_2O	H_2O	32mL

+Complete Protease inhibitor tablet (Roche)

Table 2: Dialysis Buffer (1L)

Final Concentration	Stock Solution	Amt of stock for 1L
250mM NaCl	5M NaCl	50mL
0.2mM EDTA	0.5M EDTA	400µL
10mM Tris	1M Tris pH7.9	10mL
20% Glycerol	100% Glycerol	200mL
H_2O	H_2O	740mL

Table 3: IPP Buffer (10mL)

Final Concentration	Stock Solution	Amt of stock for 10mL
250mM NaCl	5M NaCl	500µL
10mM Tris	1M Tris pH7.9	100µL
0.1% Triton X-100	10% Triton X-100	100µL
H_2O	H_2O	9.3mL

Table 4: TEV Cleavage Buffer (10mL)

Final Concentration	Stock Solution	Amt of stock for 10mL
250mM NaCl	5M NaCl	500µL
50mM Tris	1M Tris pH7.9	500µL
0.1% Triton X-100	10% Triton X-100	100µL
0.2mM EDTA	0.5M EDTA	4µL
1mM DTT	1M DTT	10µL
H_2O	H_2O	8.9mL

Table 5: Calmodulin Binding Buffer (50mL)

Final Concentration	Stock Solution	Amt of stock for 50mL
250mM NaCl	5M NaCl	2.5mL
10mM Tris	1M Tris pH7.9	500µL
0.1% Triton X-100	10% Triton X-100	500µL
2mM $CaCl_2$	1M $CaCl_2$	100µL
10mM BME	Stock BME	35µL
H_2O	H_2O	46.4mL

Table 6: Calmodulin Wash Buffer (10mL)

Final Concentration	Stock Solution	Amt of stock for 10mL
250mM NaCl	5M NaCl	500µL
10mM Tris	1M Tris pH7.9	100µL
0.1% Triton X-100	10% Triton X-100	100µL
0.1mM $CaCl_2$	1M $CaCl_2$	1µL
10mM BME	Stock BME	7µL
H_2O	H_2O	9.3mL

Table 7: Calmodulin Elution Buffer (10mL)

Final Concentration	Stock Solution	Amt of stock for 10mL
250mM NaCl	5M NaCl	500µL
10mM Tris	1M Tris pH7.9	100µL
3mM EGTA	0.5M EGTA	60µL
10mM BME	Stock BME	7µL
H_2O	H_2O	9.4mL

$CaCl_2$/mL of IgG eluate was added to the eluate from the GST column. Eluate was then transferred to a 2mL column containing 300μL of calmodulin beads and washed with 2x5mL of calmodulin binding buffer. Column was incubated on a nutator at 4°C for 2-3 hrs. Column was washed 5x with 500μL calmodulin binding buffer and then washed 2x with 500μL calmodulin wash buffer. Protein was eluted from the column with 6mL of calmodulin elution buffer. Sample was then TCA precipated by addition of TCA to a final concentration of 10% and incubated on ice for 30min. Precipitate was recovered by spinning at 13.2 kRPM at 4°C for 30 min. Pellet was washed with ice cold acetone, allowed to air dry and resuspended in 100μL 5x SDS sample buffer. Samples were separahaemolyticusted by SDS-PAGE and analyzed by silver stain.

Chapter 6

Cloning—pSSFV VopA-Flag and pSFFV VopA-C167A constructs were generated as described for chapter 4. For expression in *Yersinia pseudotuberculosis* VopA and VopA-C167A were amplified by PCR using pSFFV VopA or pSFFV VopA-C167A as template with 5`-HindII and 3`-Flag-stop-BamHI primers and cloned into pMMB67HE (a kind gift of J.B. Bliska).

Yersinia pseudotuberculosis Strains—YP126 (WT) and YP26 (ΔYopJ) were kind gifts of J.B. Bliska. For expression of pMMB67HE VopA-FLAG and pMMB67HE VopA-C167A-FLAG in YP26, the constructs were transformed into SM10λpir. Overnight cultures of SM10 strains were grown at 37°C and overnight

cultures of YP26 were grown at 26°C. 200µL of each strain were mixed and spotted onto an LB agar plate. Plates were incubated at 37°C right side up for several hours. Bacteria were scraped off of plate and plated onto M9 agar plates supplemented with ampicillin (100µg/mL) and grown at 26°C. Colonies were picked and VopA and VopA-C167A expression was verified by western blot with anti-FLAG antibody (Sigma).

Macrophage Infections—Yersinia pseudotuberculosis infections were performed as described previously (30). In brief, J774A.1 murine macrophages were seeded into 6-well dishes at a density of $1.0x10^6$ cells/mL in Dulbecco's modified eagle medium (Invitrogen) supplemented with 10% fetal calf serum (Hyclone), penicillin/streptomycin/glutamate (Invitrogen) and sodium pyruvate (Invitrogen). To induce type III secretion, overnight cultures of *Yersinia* strains were diluted back to an OD 0.1 in LB supplemented with 20mM sodium oxalate and 20mM magnesium chloride and grown at 26°}C for 1hr. Cultures were then shifted to 37°C for 2 hours. $1x10^8$ bacteria cells were pelleted and resuspended in DMEM for an MOI of 100. Bacteria were overlayed onto macrophages and plates spun at 500xg for 5 min. to bring bacteria into contact with the cells. Plates were put at 37°C for 15min and 45min. Plates were put on ice and cells were washed one time with cold PBS. Cells were lysed for 10min in radioimmunoprecipitation assay (RIPA) buffer (50mM Tris pH8.0, 150mMNaCl, 1% Nonidet P-40, 0.5% deoxycholate, 0.1% sodium dodecyl sulfate 1mM Na_3VO_4, 10mM NaF, 20mM β-

glycerophosphate, 1μM DTT, 0.5mM EGTA and complete protease inhibitor tablet (Roche)). Lysates were cleared by centrifugation at 10,000 rpm. 150μL of cleared lysate were boiled with 50μL of 5x Laemmli sample buffer. Samples were separahaemolyticusted by SDS-PAGE and analyzed by immunoblot with α-phospho Jnk and α-Jnk or α-phospho p38 and α-p38.

Epistasis Assays—HEK293T cells were transfected with or without a MAPK (HA-ERK; 200 ng) in the presence or absence of pSFFV VopA or pSFFV VopA-C167A (50 ng) with either vector, RasV12 (100 ng), Raf BxB (gift from Mike White) (10 ng) or MKK1 ED (100 ng). After 36hr of growth, cells were starved for 3 hr followed by treatment or no treatment with a stimulus (epidermal growth factor, 50 ng/ml). Cells lysates were analyzed by immunoblot with rabbit anti-phospho-ERK antibody (Cell Signaling Technology, Inc.) and mouse anti-HA antibody (Babco).

Protein purification—GST VopA WT and GST-VopA-C167A constructs were expressed in *Escherichia coli* BL21-DE3 cells and purified by GST affinity chromatography. In brief, cells were grown to *A*600 0.6–0.8 in 2x yeast extract and tryptone medium and then induced with 400 μM isopropyl-D-thiogalactopyranoside (Roche Applied Science) (IPTG) for 4 h at 25°C. The cells were lysed in phosphate-buffered saline (pH 8), 1% (v/v) Triton X-100 (Fisher), 0.1% (v/v) 2-mercaptoethanol (Bio-Rad), and 1 mM phenylmethylsulfonyl fluoride (Sigma) (PBS-T) using a cell disrupter (EmulsiFlex-C5, Avestin Inc.).

The lysates were incubated with glutathione agarose beads, and bound protein was subjected to GST-TEV cleavage overnight in PBS-T supplemented with 1mM Acetyl-CoA (Sigma) at room temperature. Flow-through was collected and incubated with GST beads to remove any remaining GST-TEV. Flow-through was collected and concentrated in a 30kDa mwco Amicon-Ultra concentrator (Fisher).

rMKK6 construct was expressed in Rosetta Blue cells (Novagen) and purified by Nickel affinity chromatography. In brief, cells were grown and lysed as above except cells were induced with 200 μ}M IPTG and grown at 25°C for 8hr. Lysates were bound to Ni^{2+}-NTA beads (Sigma). Bound protein was washed and eluted per manufacturer's protocol. His-MKK1 was expressed and purified as His MKK6 except cells were induced with 400 μM IPTG and grown at 25°C for 4hr.

In vitro Acetylation Assay—Acetylation assays were performed as described (1). In brief purified His-MKK6, His-MKK1, or p38 (a kind gift from John Humphreys) were incubated with VopA or VopA-C167A in the presence of ^{14}C labeled Acetyl CoA for 1hr at 30°C in acetylation buffer (50mM Tris pH8.0, 10%(v/v) glycerol (Fisher), 100μ}M EDTA (Fisher), 1mM Dithiothreitol (Sigma), 1 mM phenylmethylsulfonyl fluoride (Sigma)). The mixtures were resolved by SDS-PAGE, and the gels were incubated with Amplify fluorographic reagent (Amersham Biosciences) and analyzed by autoradiography.

MS method for molecular weight measurement—The protein molecular weight was measured on a Sciex QSTAR XL mass spectrometer (Applied Biosystems) with an off-line ESI source. The electrospray tips were purchased from Proxeon Biosystems. Sample solution was desalted using a Millipore C18 ZipTip and eluted with 80% ACN. The eluates were dried, then resuspended in 1 % FA, 50% ACN.

LC/MS/MS method—The tryptic digests of the sample were fractionated using a Dionex LC-Packings HPLC. Peptides were first desalted on a 300-É m x 1-mm PepMap C18 trap column with 0.1% formic acid in HPLC grade water at a flow rate of 20 É l/min. After desalting for 5 min, peptides were flushed onto a LC Packings 75 É m x 15cm C18 nanocolumn (3 É m, 100Å) at a flow rate of 200 nl/min. A 45 min gradient was used for the HPLC separahaemolyticustion, with the ACN concentration increased from 2% to 45%. Elutes were analyzed with a QSTAR XL mass spectrometer (Applied Biosystems). Data were acquired in Information Dependent Acquisition (IDA) mode where the top three precursor ions were selected per cycle for MS/MS experiment. Mass ranges for the MS survey scan and MS/MS were *m*/*z* 300–1800 and *m*/*z* 50–1800, respectively. Raw data were processed by Analyst QS to generate the PKL file. Data were searched by using Mascot search engine (Matrix Science Ltd., London, U.K.) against the SwissProt database and the home-built database, which contains the sequence of the MEKK6 protein.

Nucleotide Binding Assay—Purified His-MKK1 (1μM) was preincubated with acetyl-CoA in the presence or absence of purified VopA (50nM) or VopA-C167A (50nM) in 20mM Hepes pH 7.5 (Sigma), 10mM MgOAc and 1mM Dithiothreitol (Sigma) for 2hr at 30°C. MANT-ATP (25μM) or MANT-ADP (25μM) was added to appropriate samples. Emission scans were measured on a fluorimeter (Photon Technology, Inc.) from 300nm to 550nm with an excitation wavelength of 290nm.

Chapter 7

Cell lines and Culture Conditions—HeLa cells were routinely cultured in Dulbecco's modified eagle medium (Invitrogen) supplemented with 10% fetal calf serum (Hyclone). *V. parahaemolyticus.* strains were cultured in marine LB (luria broth with a final NaCl concentration of 3%) or heart infusion media (Gibco) at 30°C. See strain list for sources of *V. parahaemolyticus* strains.

HeLa Infections with Vibrio parahaemolyticus—For infections HeLa cells were seeded onto coverslips in 6-well dishes at a density of $2.0x10^5$ cells/mL the night before. HeLa cells were infected either with overnight cultures for 5 hours or with induced samples at varying MOIs for varying times. For induction of *V. parahaemolyticus.*, overnight cultures of *V. parahaemolyticus* cultures were diluted back to OD_{600} 0.05 in heart infusion broth and grown at 37°C for 5 hours (18). To end infection, media was removed and cells were fixed in 4% parahaemolyticusformaldehyde (Sigma). Cells were permeabilized by incubation

in TBS with 0.1% Triton-X 100. Cells were stained with Hoechst and/or rhodamine-phalloidin (Invitrogen). Coverslips were washed with PBS to remove excess stain. Coverslips were mounted with mounting media (50% glycerol and 10mg/mL n-propyl gallate in PBS) on slides and sealed with clear nail polish (Revlon). Slides were viewed on an Axio vert 200 microscope (Zeiss) images were captured with a Hamamatsu Orca-ER camera and images were viewed with OpenLab Software (courtesy of the Michelle Tallquist lab) Images were also viewed on the LSM 510 META laser scanning confocal microscope (Zeiss) and images were viewed with ImageJ software.

TCA Precipitation of Culture Supernatants—Overnight cultures were diluted back to an OD_{600} 0.01 in heart infusion media and grown at 37°C for five hours. A culture volume equal to 1 OD of cells was removed and the cells were pelleted. The culture supernatant was then filter sterilized and 66μg of BSA was added as a control for the precipitation reaction. 100% trichloroacetic acid (TCA) (Sigma) was added to the culture supernatant to a final concentration of 10%. Samples were placed at 4°C overnight. Precipitate was pelleted by centrifugation at 13,000 RPM at 4°C for 10min. Pellets were washed with ice-cold acetone. Pellets were resuspended in 100μL of SDS sample buffer. 10μL of sample were run on 12% SDS PAGE gel, transferred and western blotted with anti-VopL antibody (1:3000) (courtesy of Amy Liverman). Membranes were then stained coomassie blue stain to visualize the BSA bands.

Table 8: List of Primers

Primer	Sequence
5` HindIII VopP	5`-GAT CGT AAG CTT ATG AAA GTA AAT TTA GAA CAA AAT C-3`
3`APA Stop FLAG VopP	5`-TCG ATC GGG CCC TTA CTT GTC ATC GTC GTC CTT GTA GTC AAG ATT ATT CAA AAG ACC TTT TG-3`
VopP Eco 5`	5`-GAT CGT GAA TTC ATG AAA GTA AAT TTA GAA CAA AAT C-3`
VopP BamHI 3`	5`-TCG ATC GGA TCC TTA AAG ATT ATT CAA AAG ACC TTT TG-3`
VopA Seq1	5`-GGC ATT CAT TGT ATA GCG
VopA Seq4	5`-ACT ATC AGC ATC CTT AAC GG-3`
5` BamHI VopA	5`-GAT CGT GGA TCC ATG AAA GTA AAT TTA GAA CAA AAT C-3`
3`-VopA NcoI	5`-TCG ATC CCA TGG AAG ATT ATT CAA AAG ACC TTT TG-3`
5` BamHI TAP	5`-GAT CGT GGA TCC ATG AAG AGA AGA TGG AAA AAG AAT-3`
3` TAP XhoI	5`- TCG ATC CTC GAG TCA GGT TGA CTT CCC CG-3`
5` NcoI Tap	5`-GAT CGA CCA TGG GGT GGT GGT AAG AGA AGA TGG AAA AAG AAT-3`

Table 9: List of *Vibrio parahaemolyticus* Strains

Strain	Phenotype	Resistance	Source
LM5674	Δ*opaR*	Amp^r	L. McCarter
LM7029	LM5674 Δ*vpa1342*::Cam^r	Amp^r, Cam^r	L. McCarter
LM7035	LM5674 Δ*vp1672*::Cam^r	Amp^r, Cam^r	L. McCarter
LM7341	LM5674 Δ*vpa1342*::Cam^r, Δ*vp1672*::Kan^r	Amp^r, Cam^r, Kan^r	L. McCarter
POR-1	RIMD2210633 Δ*tdhA,* Δ*tdhS*	Amp^r, Kan^r	(31)
POR-2	POR-1 Δ*vp1662*	Amp^r, Kan^r	(18)
POR-3	POR-1 Δ*vpa1355*	Amp^r, Kan^r	(18)

Chapter Four

Inhibition of MAPK Signaling Pathways by VopA from *Vibrio parahaemolyticus*

Introduction:

V. parahaemolyticus is phylogenetically close to *Vibrio cholerae* (the causative agent of cholera), and recent sequencing of the *V. parahaemolyticus* genome reveals the existence of two pathogenicity islands (PAI and PAII), which are not found in *V. cholerae* (3). Encoded within PAII is a type III secretion system and an effector protein, referred to as VopA, sharing 55% similarity with the YopJ-like proteins from *Yersinia* and *Salmonella* (3). YopJ-like effectors are expressed by a number of bacteria, including pathogens, commensals, and symbionts. These effector proteins, like other type III secreted virulence factors, are expressed by the bacteria and injected into the target host cell where they manipulate the host machinery.

Our studies reveal that VopA, encoded by *V. parahaemolyticus*, is able to manipulate eukaryotic signaling machineries, and may be used during its existence as a commensal or incidental pathogen. Herein, we observe that VopA functions in a mechanistically similar manner to other YopJ-like proteins but demonstrates a remarkable diversity in its inhibitory profile of signaling pathways.

Results:

Lack of Inhibition of NFκB Pathway by VopA—We examined whether *Vibrio* VopA is able to inhibit the induction of innate immune response by blocking the NFκB pathway in a manner similar to other YopJ-like effector proteins (22,32). Wild-type YopJ and VopA and the catalytically inactive forms of these effectors (YopJC172A or VopAC167A) along with FLAG-tagged IκB were transfected into 293T cells or HeLa cells and then stimulated with either TNFα or interleukin-1β, respectively. Surprisingly, VopA demonstrated no inhibitory activity on the NFκB signaling pathway. Neither wild-type VopA nor the catalytically inactive VopAC167A is able to inhibit the phosphorylation of IκB with either stimulus (TNFα or interleukin-1β) (Fig. 10, *A* and *B*, respectively). In NFκB luciferase reporter assays, VopA is unable to inhibit TNFα-induced activity. Taken together, these observations support the hypothesis that VopA has no effect on the NFκB pathway, which is in contrast to the two other YopJ-like effectors from animal pathogens, YopJ and AvrA.

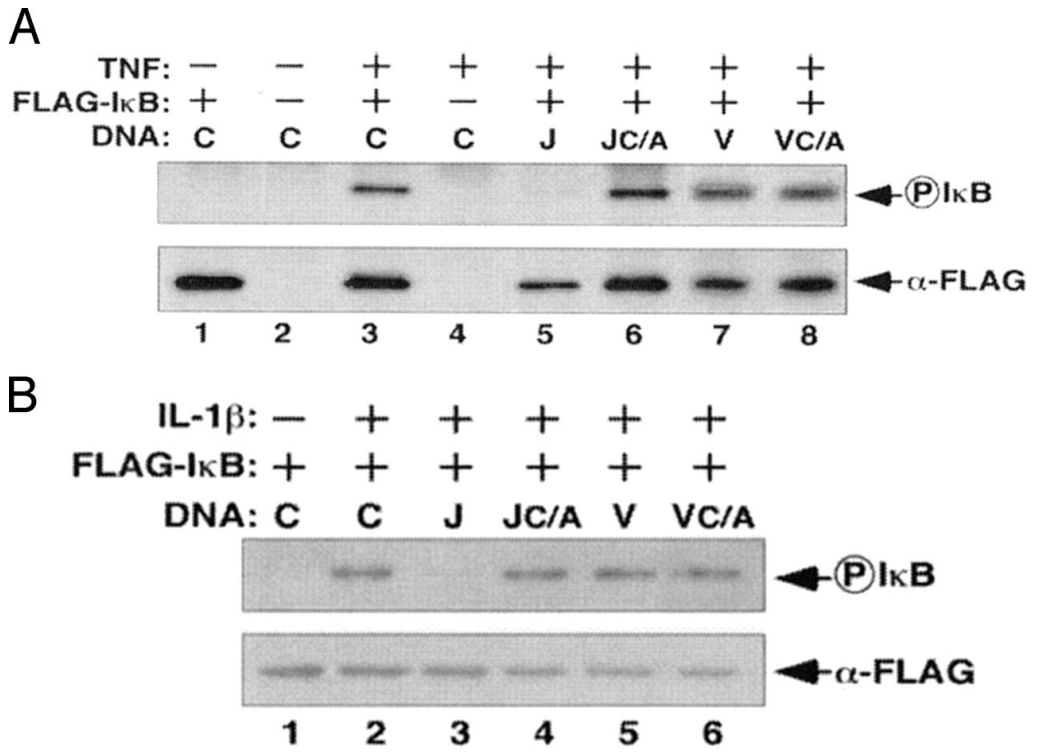

Figure 10: Effect of *Vibrio* VopA expression on the NFκB pathway. *A*, 293T cells transfected with or without FLAG-IκB in the presence or absence of YopJ-like effector plasmids and treated with TNFα were assayed for IκB phosphorylation. *B*, HeLa cells were transfected as described in *A* but were treated with interleukin-1β (*IL-1β*). *C*, control vector; *J*, YopJ; *JC/A*, YopJ C172A; *V*, VopA; *VC/A*, VopA-C167A.

VopA Inhibits the Mammalian MAPK Pathways—Yersinia YopJ is able to inhibit MAPK signaling pathways, so we next assessed the ability of *Vibrio* VopA to inhibit the mammalian MAPK pathways. 293T cells were transfected with various YopJ-like effectors in the presence of HA-ERK followed by treatment with epidermal growth factor (22). Both wild type YopJ and VopA, but not the catalytically inactive forms of these effectors (YopJC172A or VopAC167A), are able to inhibit extracellular growth factor-induced ERK activation (Fig. 11*A*). In a similar fashion, both YopJ and VopA are able to inhibit the other MAPK pathways. These studies provide the first evidence that *Vibrio* VopA is able to inhibit mammalian signaling pathways. The various YopJ-like effectors appear to target distinct sets of signaling pathways within the eukaryotic cell. However they would appear to have unique targets within these signaling pathways. For example, in contrast to YopJ, no interaction is observed between VopA and the family of MAPK kinases in yeast two-hybrid binding assays.

Both YopJ and VopA are very efficient at inhibiting the MAPK pathways, but detecting the expression of these YopJ-like proteins is extremely difficult (Fig. 11*A*). To determine the potency of inhibition by these effectors, we analyzed their MAPK inhibitory activity over a range of expression conditions. Inhibition of the MAPK signaling pathway is observed with as little as 1 ng of YopJ- or VopA-transfected DNA. Although the inhibition of the MAPK pathways is

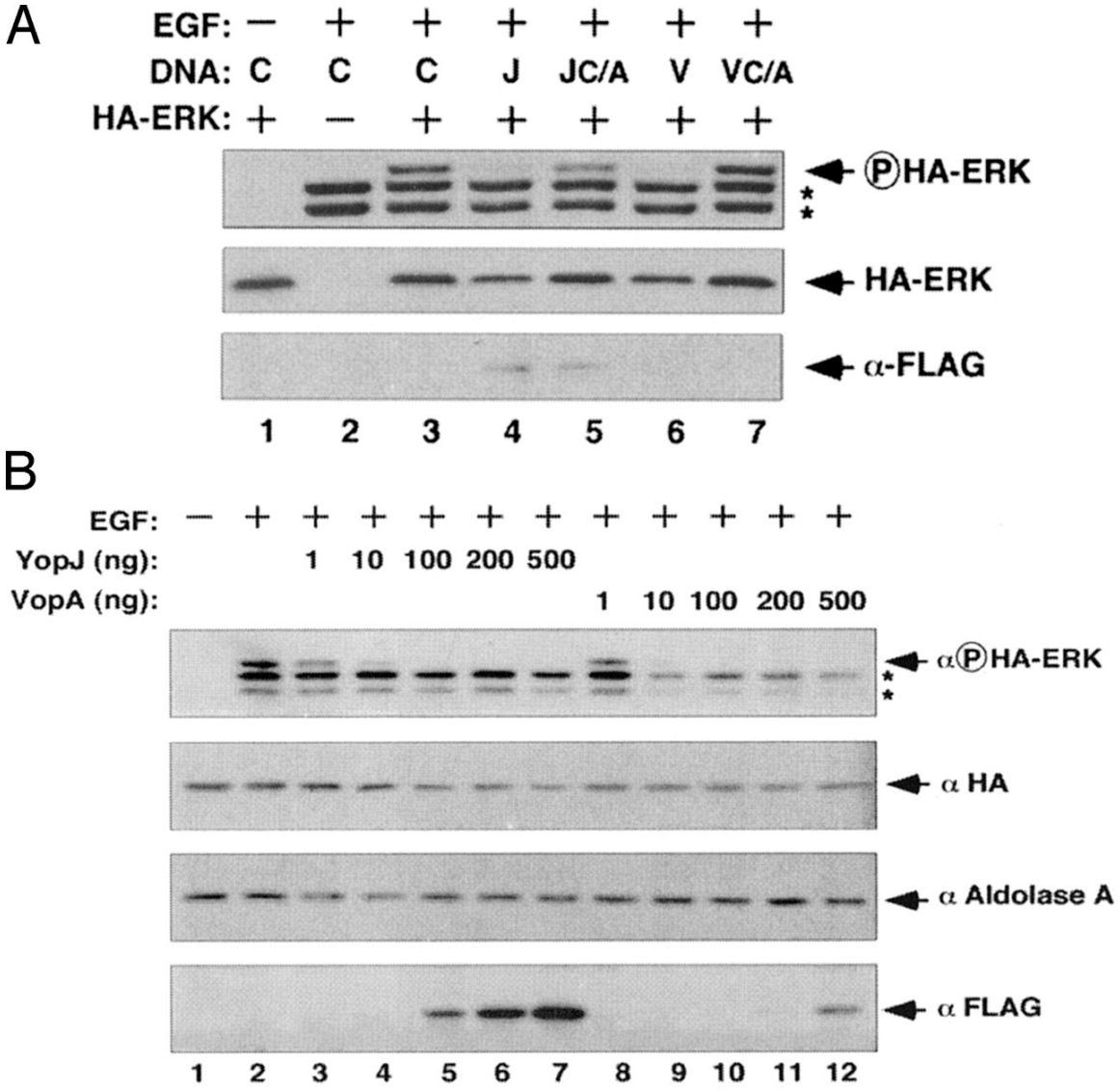

Figure 11: Inhibition of MAPK pathway by *Vibrio* VopA. *A*, 293T cells transfected with or without HA-ERK in the presence or absence of YopJ-like effector plasmids were assayed for HA-ERK activation. *Asterisks* indicate endogenous phospho-ERK1,2. YopJ-like protein is detected using anti-FLAG (Sigma). *B*, inhibition of the MAPK pathway with indicated amounts of YopJ and VopA was performed as described in *A*. Immunoblotting with Aldolase A is used as a loading control. *EGF*, extracellular growth factor; *C*, control vector; *J*, YopJ; *JC/A*, YopJ C172A; *V*, VopA; *VC/A*, VopA-C167A.

comparable between the two effectors, the amount of YopJ-FLAG protein appears to be at least 10-fold greater than that of VopA-FLAG (as detected by anti-FLAG immunoblots) (Fig. 11*B*).

The Role of VopA in Programmed Cell Death—Having established a profile of inhibitory activity for these YopJ-like effectors, we wanted to investigate what role these effectors (independent of other pathogenic factors) play on the fate of an infected cell. We utilized the well-established system in lymphoma cells whereby TNFα-induced apoptosis is prevented by the induction of the NFκB pathway resulting in the expression of anti-apoptotic factors (33,34). Effectors were transfected into Jurkat cells and following stimulation with TNFα, were assessed for survival (Fig. 12). Cell death was not observed in control cells in the presence or absence of stimulus. Wild-type YopJ, but not the catalytically inactive form of YopJ, is able to efficiently promote cell death in Jurkat cells but only in the presence of stimulus, which supports the hypothesis that the *Yersinia* YopJ effector does not directly activate death machinery but promotes cell death by the blocking of signaling pathways. The ability of VopA to promote cell death in the presence of stimulus is marginal (Fig. 12) and cannot be attributed to blocking the NFκB pathway but may result as an indirect consequence of its extremely potent inhibition of the MAPK pathways.

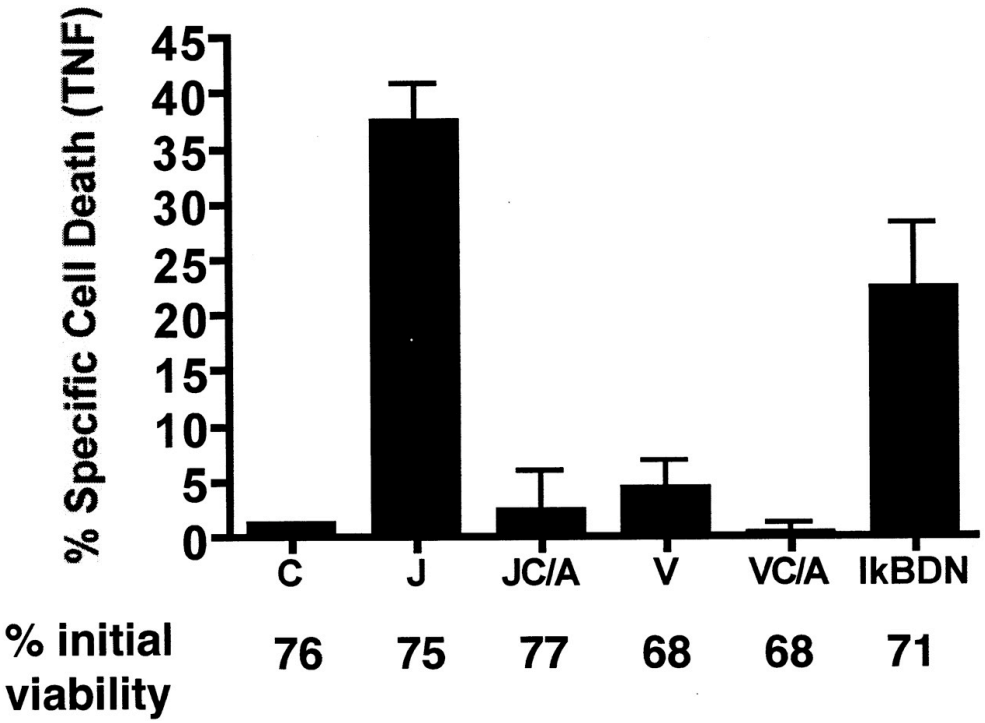

Figure 12: Induction of cell death by YopJ and VopA. Jurkat cells were transfected with indicated plasmids and 24 h later stimulated or not with 100 ng/ml TNFα for 12 h. The % ± S.E. specific cell death of TNFα-treated *versus* control cells is shown. Data are representative of four independent experiments. Spontaneous cell death of cells transfected with any of the YopJ homologuess was always less than 10%. Percent of initial viability with indicated expression vector is listed under each experiment. *C*, control vector; *J*, YopJ; *JC/A*, YopJ C172A; *V*, VopA; *VC/A*, VopA-C167A; *IκBDN*, IκB dominant negative.

Expression of VopA in Yeast Causes a Growth Arrest Phenotype — One of the characteristics of bacterial pathogenic effectors secreted by a type III secretion system is that their usurped eukaryotic activities are evolutionarily conserved. Studies with *Saccharomyces cerevisiae* expressing a galactose-inducible YopJ plasmid demonstrated that the mechanism used by YopJ to inhibit the MAPK signaling pathways is evolutionarily conserved (25). To initially test the effect that VopA has on the MAPK pathways in yeast, strains containing this effector and its mutant counterpart, under the control of a galactose-inducible promoter, were grown to mid-log phase in glucose media followed by plating onto glucose or galactose media. When yeast cells containing VopA plasmid are plated on galactose, thereby inducing the expression of VopA, the yeast cells are unable to grow (Fig. 13*D*). In contrast, yeast cells expressing the catalytically inactive VopAC167A are able to grow on galactose media. Yeast cells expressing VopA when scraped off the galactose plates are able to recover and grow when plated on glucose plates, supporting the idea that the catalytic activity of the *Vibrio* effector, VopA, induces a growth arrest phenotype (data not shown).

Using liquid growth culture studies, we observed the effects on the growth of yeast cells expressing various forms of YopJ-like proteins. Yeast cells containing a control vector or vector expressing YopJ, YopJ C172A, or VopA-C167A grow at approximately the same rate (Fig. 13*B*). In contrast, the growth of VopA-expressing yeast cells is dramatically hindered, but they continue to grow,

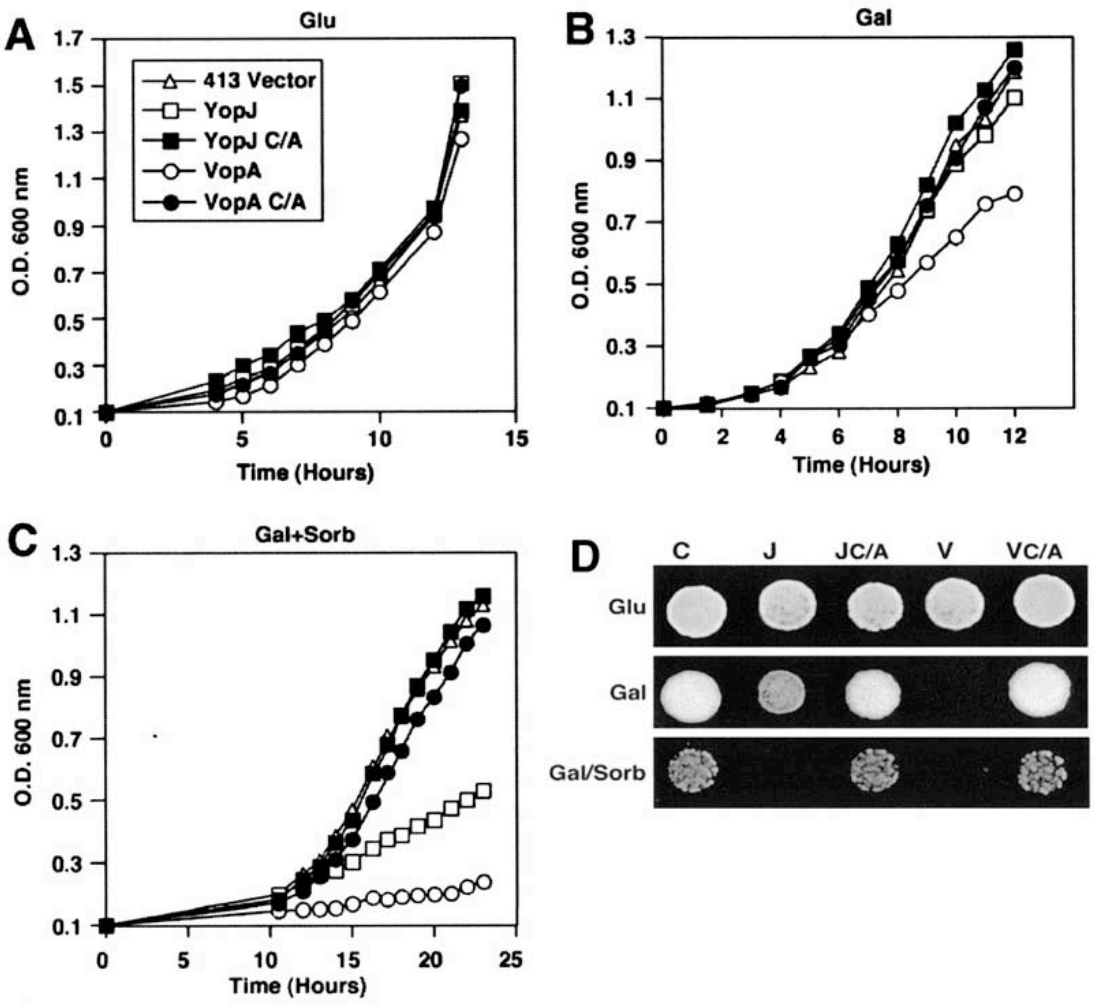

Figure 13: *Vibrio* VopA inhibits growth when expressed in yeast. Growth assay demonstrates the effect of effector expression on growth in liquid media containing glucose (*Glu*) (*A*), galactose (*Gal*) (*B*), and galactose with 1 M sorbitol (*Gal Sorb*) (*C*). *D*, growth assay demonstrates the effect of effector expression on yeast growth on media containing glucose, galactose, and galactose with 1 M sorbitol. Data shown are representative of three experiments.

albeit at a slower rate than the other strains (Fig. 13*B*). In cells expressing VopA, growth arrest is observed over an extended period of time, indicating that the growth arrest is not likely to be a cell cycle-dependent defect. The phenotype is dependent on wild-type VopA and not the catalytically inactive form of VopA, indicating that the mechanism of inhibition is similar to other YopJ-like effectors but that the targets are distinct.

Inhibition of MAPK Pathways by VopA Is Evolutionarily Conserved—To investigate whether VopA, like YopJ, inhibits MAPK signaling pathways in yeast, cells containing the various effectors were plated on galactose media with 1 M sorbitol, which results in the activation the high osmolarity growth (HOG) MAPK pathway (25). As expected, yeast expressing either YopJ or VopA, but not the catalytically inactive mutants, plated on galactose media containing 1 M sorbitol are unable to grow (Fig. 13*D*). Consistent with our observations in mammalian systems, *Salmonella* AvrA shows no obvious inhibitory effect on the MAPK pathways in yeast (data not shown). When yeast expressing YopJ or VopA are grown in liquid media containing 1 M sorbitol, the growth phenotype is quite striking (Fig. 13*C*). Growth is almost immediately arrested in the presence of VopA, whereas in the presence of YopJ, the growth arrest requires more time. These observations further emphasize the difference in targets between YopJ and VopA and indicate that the growth arrest phenotype in the presence of VopA does not depend only on the inhibition of the activated HOG MAPK pathway.

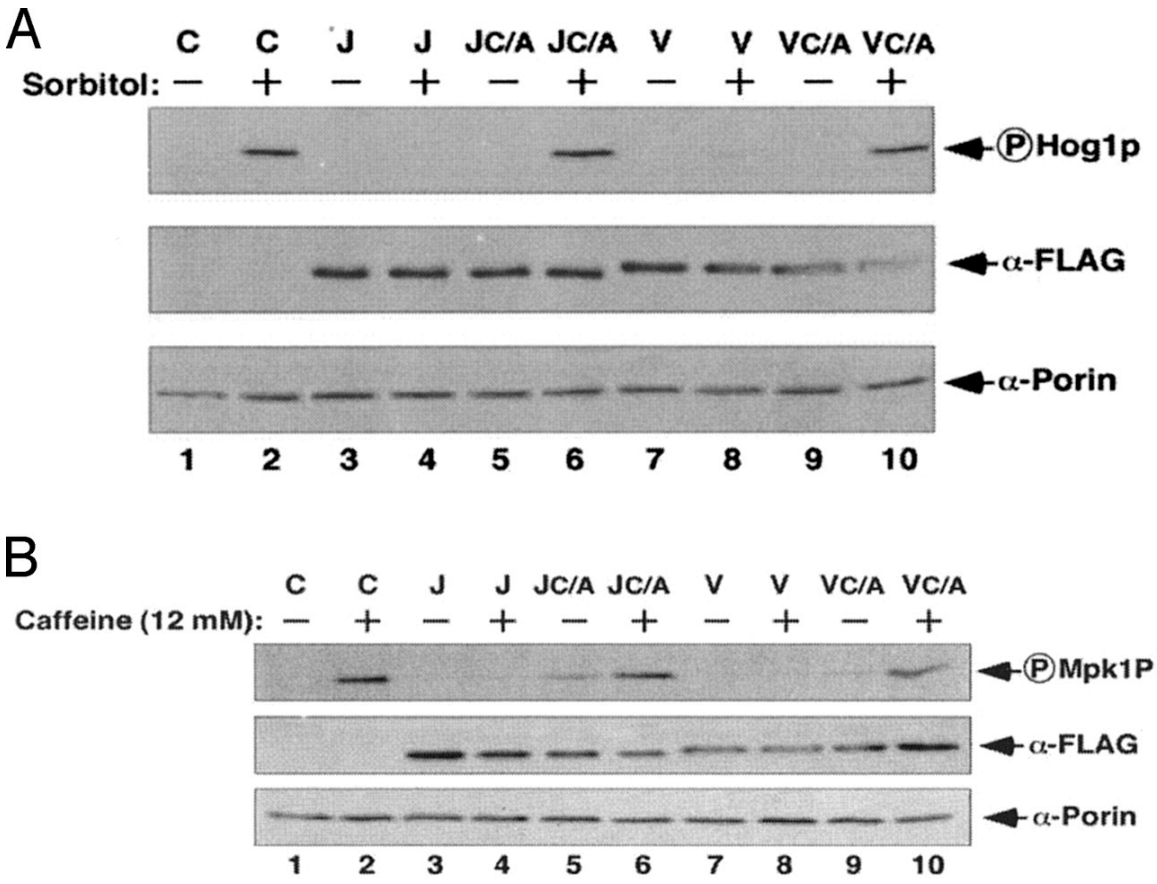

Figure 14: *Vibrio* VopA inhibits MAPK signaling when expressed in yeast. The ability of YopJ and VopA to inhibit activation of the yeast MAPKs Hog1p and Mpk1p is assayed by inducing cells with either 0.7 M sorbitol for 2.5 min (*A*) or 12 mM caffeine for 1 h (*B*). *C*, control vector; *J*, YopJ; *JC/A*, YopJ C172A; *V*, VopA; *VC/A*, VopA-C167A.

To test the ability of VopA to inhibit the HOG MAPK pathway, yeast cells were grown in glucose media to mid-log phase and then transferred to galactose media to induce expression of the YopJ-like proteins. These cells were incubated with sorbitol, and the lysates of cells were analyzed for induction of the HOG MAPK pathway (25). Yeast cells containing either a control vector or the plasmids encoding catalytically inactive forms of YopJ or VopA are able to activate Hog1p via phosphorylation, whereas wild-type YopJ and VopA inhibit Hog1p activation (Fig. 14*A*). Similar results are observed using caffeine to induce the cell wall integrity MAPK pathway (35); yeast cells expressing wild-type YopJ or VopA, but not their mutant counterparts, are unable to induce the activation of Mpk1p via phosphorylation in this pathway (Fig. 14*B*). VopA, like YopJ, inhibits evolutionarily conserved MAPK signaling pathways in yeast, but unlike YopJ, demonstrates the ability to induce a growth arrest phenotype in yeast indicating a distinct set of targets for VopA.

Discussion:

The profiles of inhibition for each of the mammalian YopJ-like effectors are clearly distinct. VopA potently blocks the evolutionarily conserved MAPK pathways, YopJ blocks MAPK pathways and the NFκB pathway (22), and AvrA blocks only the NFκB pathway (32) (Fig. 15*A*). Each pathogen has evolved to encode a YopJ-like effector that displays a unique inhibitory activity but requires a common catalytic site (Fig. 15*B*) that benefits its respective pathogen in

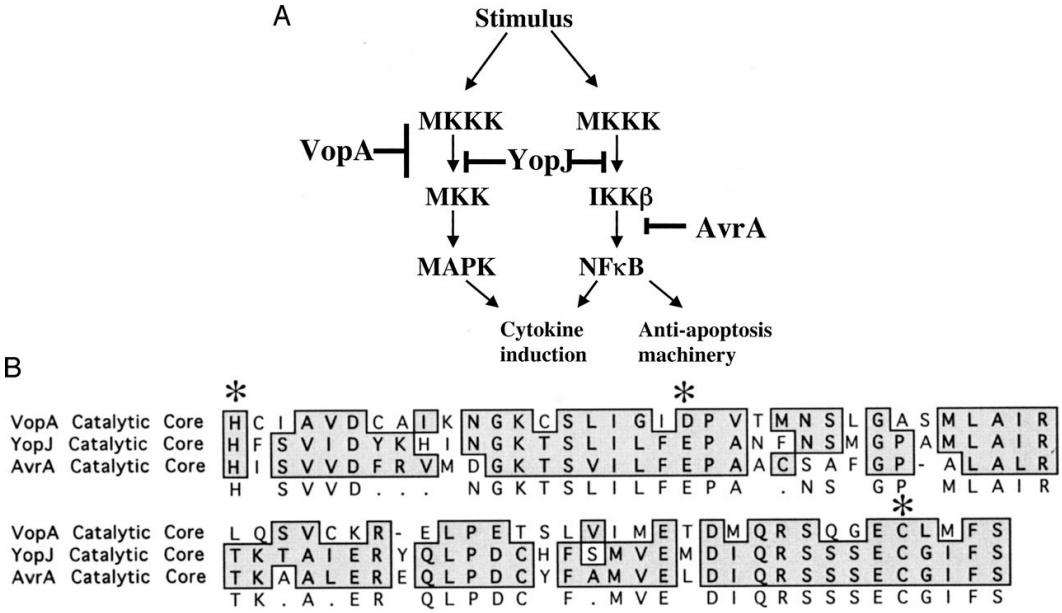

Figure 15: Comparison of YopJ proteins. *A*, model depicting the various inhibitory activities of *Yersinia* YopJ, *Vibrio* VopA, and *Salmonella* AvrA on mammalian signaling pathways is shown. *B*, alignment of the catalytic core of VopA, YopJ, and AvrA is shown. *Asterisks* designate catalytic residues. *MKK*, MAPK kinase; *MKKK*, MAPK kinase kinase; *IKK*, IκB kinase.

different ways. The activity of *Yersinia* YopJ complements its fellow effectors by blocking the production of cytokines and anti-apoptotic machinery, thereby preventing the induction of the innate immune response and promoting apoptosis. *Salmonella* AvrA does not affect MAPK signaling in mammalian cells or yeast but does inhibit the NFκB pathway (32), albeit weakly, and does abrogate the constitutive degradation of β-catenin (36). This inhibitory activity results in c-Myc-induced proliferation of the infected cell, which may prolong the life of the infected cell and allow for propagation of an intracellular pathogen (36). *Vibrio* VopA, which we have shown to be an extremely potent inhibitor of the evolutionarily conserved MAPK pathways, may function to inhibit cytokine production resulting in attenuation of the host defense response. The activity of VopA along with other virulence factors could facilitate colonization in the intestine of humans resulting in propagation of the pathogen. Alternatively, VopA may by used to attenuate signaling while existing as a commensal in the shellfish host. Currently, only laborious animal models (*e.g.* the ligated rabbit ileal loop model) exist for studying *V. parahaemolyticus* (9), but systems to study infection by *V. parahaemolyticus* using a tissue culture-based approach are currently being developed.

In summary, three different types of intestinal pathogens have usurped a structurally conserved and mechanistically similar activity in the form of a YopJ-like effector. The catalytic domain of this molecule may then have been

transformed into a unique activity that is maintained and used by a specific pathogen for targeting and inhibiting a distinct set of signaling pathways for the advantage of the pathogen during infection of the host. As YopJ effectors are maintained and expressed by both plant and animal pathogens as well as a plant symbiont (and most likely in yet to be discovered animal commensals), they provide powerful tools for identifying critical steps in eukaryotic signaling machineries that are important for host response and survival during infection and/or symbiosis.

Chapter Five

The Hunt for VopA's Targets

Introduction

VopA is a close homologue of the *Yersinia* effector YopJ. Initial characterization of YopJ involved identification of binding partners via two-hybrid analysis. The binding partners identified in this screen, mainly family member of the MAP Kinase Kinase superfamily, reflected the pathways affected by YopJ (22). We showed that VopA is able to inhibit the MAPK pathway but does not affect the NFκB pathway. VopA's ability to inhibit growth in yeast while YopJ does not implies additional targets in the cell other than MAPK. In attempts to identify VopA's binding partners I used a two-pronged approach. First, I attempted a genetic approach using a yeast two-hybrid system (29). I then used biochemical approaches that included GST pulldown experiments and a tandem affinity purification (TAP) protocol (37).

Results and Discussion

Yeast Two-Hybrid Screen Trial One—To identify potential binding partners of VopA, full-length VopA was cloned in frame into the yeast two hybrid bait plasmid pLexAde. This construct was transformed into the two-hybrid bait strain L40, which contains two integrated reporters *his3* activation and a LacZ reporter. The bait strain was then transformed with a HeLa cDNA library and plated onto YCD-WHULK plates to select for bait and library plasmid pairs that activate the

his3 reporter. 370 positives were obtained and restreaked onto YCD-WHULK. After multiple passages on YCD-WHULK positives were tested for β-galactosidase activity. Of the 370 positives, 100 were positive for induction of the LacZ reporter.

Library plasmids were then segregated from the bait plasmid by streaking on YCD-L media with low adenine. The L40 strain contains a defect in *ade2* that is complemented by the bait plasmid pLexAde. In the absence of pLexAde colonies turn pink in the presence of low adenine due to accumulation of an adenine precursor. After several passages on YCD-L, strains were tested on YCD-WL to test for presence of bait plasmid. Once strains containing only the library plasmid were obtained these strains were then tested for autoactivation by mating with a strain containing an empty bait plasmid, for nonspecific binding by mating with a strain containing the bait plasmid expressing lamin and for VopA binding by mating with the original bait plasmid, pLexAde VopA. Of the 100 positives tested none were found to recapitulate *his3* activation in the presence of VopA. These results indicate that the positives identified were either false-positives or had only a weak affinity for VopA.

Yeast Two-Hybrid Screen Trial Two—For this trial the same system was used for the two-hybrid screen including the bait construct and strain. Instead of the HeLa cDNA library used in the previous screen I used a rat brain cDNA library (courtesy of Eric Olson's lab). From this screen 288 positives were obtained and

restreaked onto YCD-WHULK. After multiple passages on YCD-WHULK positives were tested for β-galactosidase activity. Of the 288 positives, 87 were positive for induction of the LacZ reporter.

The library plasmid was segregated and these strains were mated with two strains: one with the empty bait plasmid to test autoactivation and one with bait plasmid expressing lamin to test for specificity of interactions. All of the putative positive strains mated with the control plasmid strain appeared active in the β-galactosidase assay. These results along with the results from the previous two-hybrid screen indicate that VopA most likely does not bind its targets too tightly, which in the context of catalytic activity is beneficial for turnover.

GST pulldown from HeLa Lysate—As a complement to the genetic approach for finding targets of VopA biochemical approaches were also utilized. GST-VopA expresses at high levels in bacterial cells and can be easily purified to a high level of purity. This protein was used in pulldown experiment with HeLa lysates. HeLa lysates were prepared by lysis in TX buffer. This is a gentle lysis that should maintain signaling complexes in the cell. Intact signaling complexes could be required for VopA binding. For this assay HeLa lysates were incubated with either GST or GST-VopA bound to glutathione sepharose (GST-beads or GST-VopA beads). Silver stained samples showed the presence of two additional bands at approximately 200kDa and 40kDa that bound to GST-VopA beads but not GST beads. (Figure 16). These bands were sent for identification at the mass

spectrometry core. The 200 kDa band was identified as filamin-1 and the ~40 kDa was identified as actin. Filamin-1 is an actin binding protein that is involved in coordinating the actin cytoskeleton and is involved in the formation of 90 degree turns in the actin cytoskeleton. It is also able to serve as a scaffolding protein for signaling cascades related to actin rearrangement (38). Attempts to confirm the interaction between VopA and filamin-1 via reverse pulldown with anti-filamin antibody failed. Other experiments to verify interactions with actin also failed. The inability to recapitulate the interaction with either filamin-1 or actin indicates that these could have been artifacts of the GST pulldown.

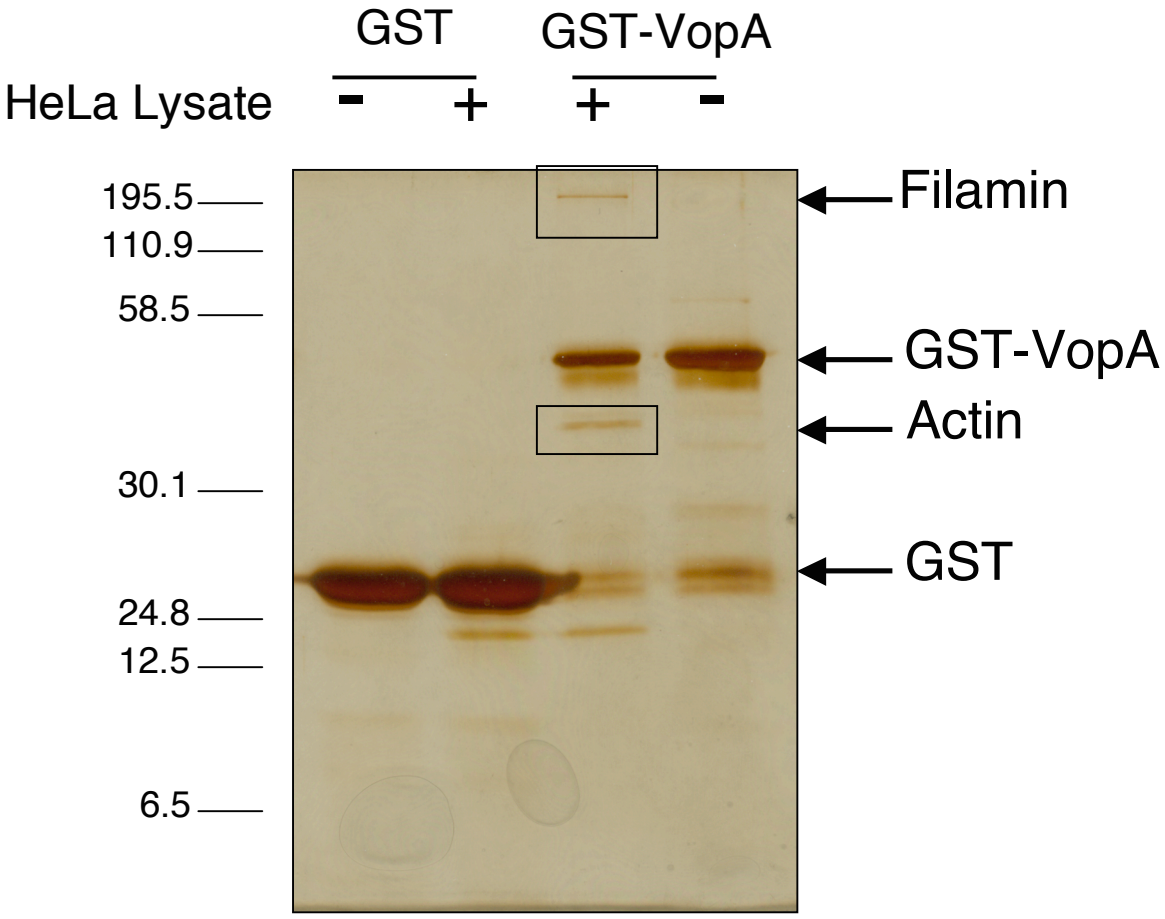

Figure 16: GST-VopA Pulldown with HeLa Lysate. A silver stained SDS-PAGE gel showing the results of the pulldown. Boxes indicate the bands unique to the GST-VopA with HeLa lysate lane. The large band was identified as Filamin and the smaller band was identified as actin.

TAP-Tag Purification—The tandem affinity purification (TAP) tag is a purification tag designed as a generic system for obtaining highly purified complexes from yeast and mammalian cells (37). The TAP-tag consists of two affinity tags, protein A and calmodulin binding peptide connected by a linker with a TEV protease site. In the first step of purification the components of the complex are bound to IgG beads, washed and then released by TEV cleavage (Fig. 17). In the second step of purification the cleaved protein is bound to calmodulin beads in the presence of calcium (Fig. 17). This allows for gentle elution conditions with no extreme changes in pH or salt concentrations that could disrupt the purified complex. The purified complex is then TCA precipitated and analyzed by SDS-PAGE and the components can then be identified by mass spectrometry. This approach was utilized with VopA to try to eliminate any potential artifacts similar to what was found from the GST pulldowns. TAP-VopA was expressed in yeast under a galactose inducible promoter to counter the VopA effect on yeast growth. TAP-VopA was purified via this method. Although, VopA was purified to a high level of purity unfortunately there were no additional proteins that copurified with the VopA (Figure 18). The purification was attempted under multiple salt conditions but unfortunately no additional proteins were copurified. This could be because, as with the two-hybrid screens, the affinity of VopA for its targets is not high enough to to maintain the protein-protein interactions through the entire purification process. Another reason could be that the proteins that interact with VopA were expressed at too low a level to be detected by silver stain.

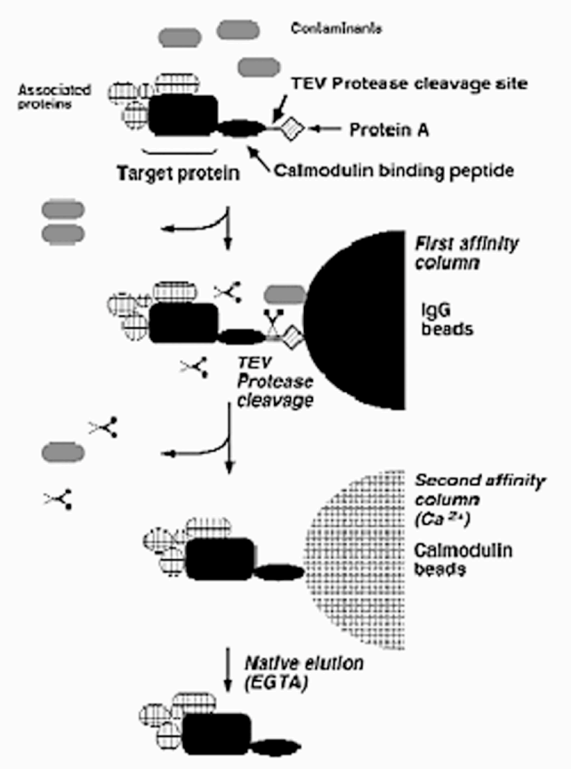

Figure 17: Overview of the TAP Purification Scheme

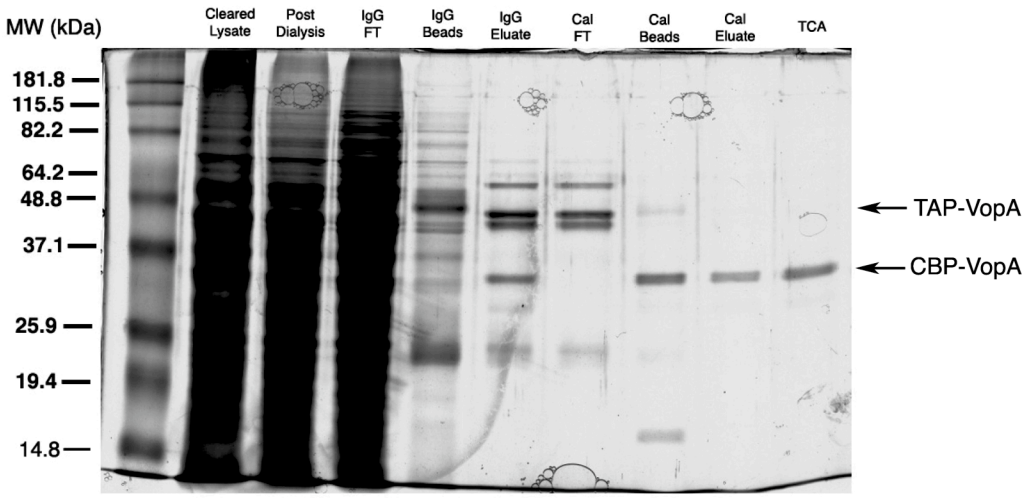

Figure 18: Purification of TAP-VopA from BY4741. A silver stained SDS-PAGE showing the purification of VopA from yeast. The upper arrow indicates the full-length TAP-VopA protein and the lower arrow indicates the cleaved VopA protein with the calmodulin binding peptide tag (CBP-VopA).

Chapter Six

VopA Inhibits ATP-binding by Acetylating the Catalytic Loop of MKKs

Introduction:

All YopJ-like proteins contain a catalytic triad and recently it was shown that YopJ functions as an acetyltransferase (1,28,39). It has been speculated that other members of the family of YopJ-like proteins might also possess this activity (28). YopJ was demonstrated to inhibit the MAPK and NFκB signaling pathways by acetylating the critical serine and threonine residues found on the activation loop of MAPK kinases thereby blocking their activation by phosphorylation (1,28,39). VopA and YopJ share ~55% similarity at the amino acid level although they inhibit signaling in different ways (40). VopA inhibits MAPK signaling using a novel mechanism distinct from those described for other bacterial toxins that disrupt this signaling pathway. This effector potently inhibits MAPK signaling but shows no inhibitory effect on the NFκB pathway (40). Herein, we show that VopA acetylates a conserved lysine located in the catalytic loop of all kinases that plays a critical role in the binding of the γ-phosphate of ATP. Modification of this lysine by acetylation inhibits the binding of ATP, but not ADP, to the MAPK kinase, resulting in an inactivated kinase. These findings uncover a unique mechanism that targets a critical conserved lysine residue involved in coordinating nucleotide binding that could also be used by eukaryotic enzymes.

Results:

VopA Inhibits Mammalian MAPK Activation—Previously we have shown that VopA is able to inhibit the ERK MAPK signaling pathway in mammals and the High Osmolarity Growth (HOG) pathway in yeast (40). To confirm that VopA inhibits other mammalian MAPK pathways, we analyzed the activation of the p38-MAPK and JNK-MAPK pathways by assessing the phosphorylation of p38 and JNK in the presence and absence of VopA or the catalytically inactive form of VopA (VopA-C167A) where the catalytic cysteine is mutated to an alanine (Fig. 19). For this analysis, VopA or VopAC167A was cloned into the bacterial expression vector, pMMB67HE, and conjugated into a *Yersinia pseudotuberculosis* strain that is deleted for YopJ (30). These strains were used to infect J744A.1 murine macrophages to test VopA's ability to rescue the deleted YopJ strain by restoring the inhibition of the p38 or JNK pathways. Infection with the wild type *Yersinia* strain that contains YopJ efficiently inhibits both the p38 and JNK MAPK pathways (Figure 19A lanes 2,3 and 19B lanes 2,3, respectively), whereas the *Yersinia* strain deleted for YopJ does not inhibit these signaling pathways (Figure 19A lanes 4,5 and 19B lanes 4,5, respectively) (30). Inhibition of the p38 and JNK phosphorylation were restored in the YopJ deletion strain by induced expression of VopA (Figure 19A lanes 8,9 and 19B lanes 8,9, respectively), but not the catalytically inactive VopA-C167A (Figure 19A lanes 12,13 and 19B lanes 12,13, respectively).

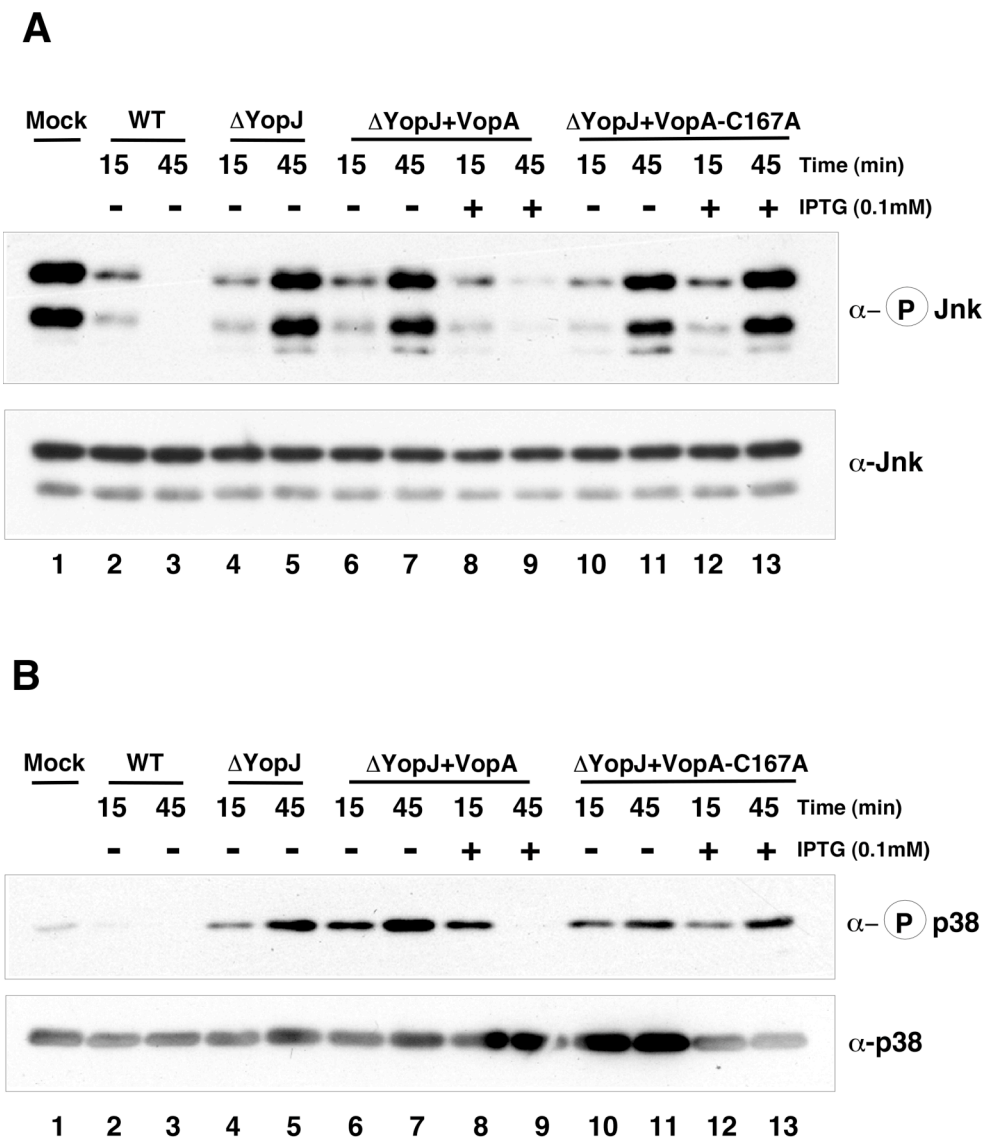

Figure 19: VopA Inhibits JNK and p38 Activation. *A,* Inhibition of JNK signaling. J774A.1 murine macrophages infected at an MOI 50 with *Yersinia pseudotuberculosis* strains overexpressing VopA and VopA-C167A and assessed for phosphorylation of JNK by immunoblot (upper panel). Immunoblot for total JNK in the lower panel shows equal loading. *B*, Inhibition of p38 signaling. Same as in *A* except assessed for phosphorylation of p38 (upper panel) and total p38 in the lower panel shows equal loading.

VopA Inhibits Downstream of MKK Activation—To determine the point at which VopA blocks the MAPK pathway, we performed a series of epistasis experiments. Consistent with previous findings, when the MAPK pathway is stimulated with an external stimulus (such as EGF) VopA, but not VopA-C167A is able to inhibit the ERK-MAPK pathway as demonstrated by the lack of phosphorylated HA-ERK in treated cells (Figure 20A) (40). Phosphorylation of endogenous ERK is observed due to the background from non-transfected, stimulated cells (Figure 20A) (40). Constitutive activation of this pathway by transfected RasV12 or B-Raf BxB is also inhibited by wild-type VopA, but not mutant VopA-C167A, as demonstrated by analysis of ERK phosphorylation (Figure 20B, 20C, respectively). Surprisingly, when an activated form of MKK1, MKK1-ED, is used to activate the pathway just upstream of ERK, VopA is still able to inhibit phosphorylation of HA-ERK (Figure 20D). This observation is in contrast to the inhibitory profile of YopJ, which is unable to inhibit signaling in the presence of an activated MKK (22). Based on these findings, we concluded that VopA inhibits MAPK signaling downstream of MKK1 activation and upstream of ERK activation.

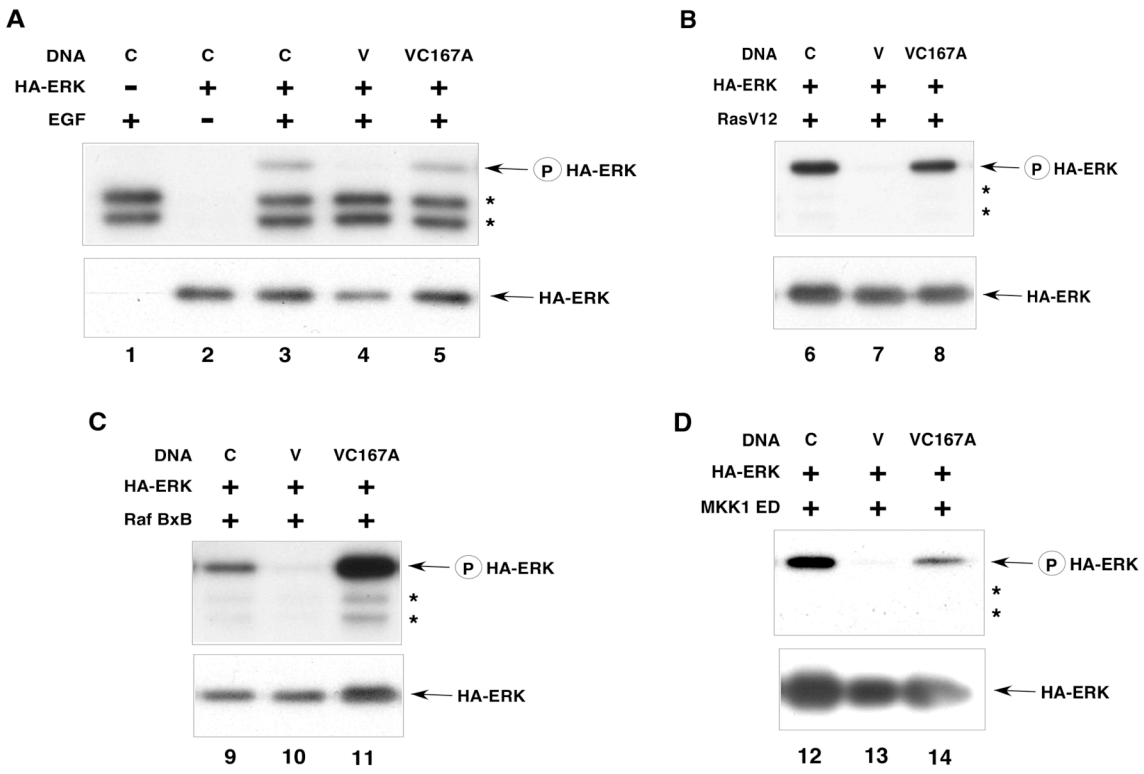

Figure 20: VopA Inhibits MAPK Signaling Downstream of MKK . *A*, 293T cells transfected with or without VopA or VopA-C167A were assayed for the ability to activate HA-ERK with an EGF (50ng/mL) stimulus. Samples were assessed for ERK activation and immunoblot with anti-HA shows equal loading of HA-ERK (lower panel). C is control DNA, V is VopA and VC167A is VopA-C167A. Asterisks denote endogenous ERK. *B*, Same as in *A* except with transfected RasV12 (10ng) as stimulus. *C,* Same as in *A* except with transfected Raf BxB (100ng) as stimulus. *D*, Same as in *A* except with transfected MKK1 ED (100ng) as stimulus.

VopA Acetylation of MKK6 Inhibits Activation—Given that VopA only affects the MAPK signaling pathways and that it also inhibits the activation of MAPKs, we predicted the molecular target of VopA would be MAPKs (40). In addition, due to the fact that VopA is a member of the family of YopJ-like proteins and that YopJ is an acetyltransferase, we hypothesized that VopA functions as an acetyltransferase that acetylates and inhibits MAPK activation (28). To test this hypothesis, we used purified p38 in an *in vitro* acetylation assay with purified wild type and mutant VopA. However, we observed that neither VopA nor the catalytically inactive VopA-C167A acetylates p38 (Figure 21A). However, as a control we included rMKK6 as a substrate and discovered that VopA, but not mutant VopA-C167A, is able to acetylate rMKK6. Previously, YopJ was observed to acetylate rMKK6 on its activation loop, thereby preventing phosphorylation by upstream kinases (1,39). To determine if VopA is modifying rMKK6 in a similar manner, we tested whether rMKK6 is phosphorylated by upstream kinases in the presence or absence of VopA using a previously established *in vitro* signaling assay (1). rMKK6 is preincubated with GST-VopA or GST-VopA-C167A in the presence or absence of acetyl-CoA, followed by incubation with membrane-free lysates derived from serum stimulated cells. In control samples without VopA, rMKK6 is phosphorylated and activated by upstream kinases as indicated by immunoblot analysis with an anti-phospho-MKK6 antibody that recognizes the phosphorylated residues on the activation

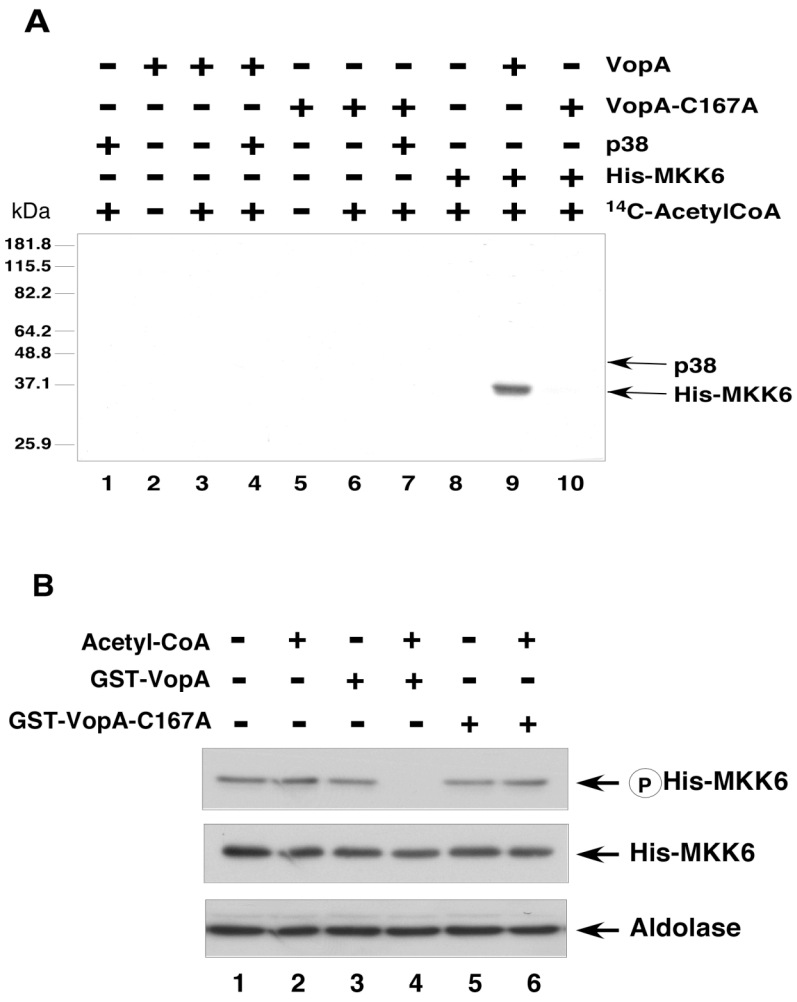

Figure 21: VopA Acetylates MKK and Inhibits Activation. *A*, VopA acetylates rMKK6. Recombinant p38 or His-MKK6 and recombinant VopA WT or VopA-C167A were incubated in the presence of ^{14}C labeled acetyl-CoA. Proteins incubated only with ^{14}C labeled acetyl-CoA were used as controls. Acetylation of samples was analysed by SDS-PAGE followed by autoradiography. *B*, VopA's acetylation of rMKK6 inhibits activation. rMKK6 was preincubated alone or with VopA or VopA-C167A in the presence or absence of acetyl-CoA. rMKK6 was then activated by addition of HeLa cell-free lysates. Activation was detected by immunoblot (upper panel). α-His shows equal loading of His-MKK (middle panel) and α-aldolase (lower panel) shows equal loading of lysate.

loop (Figure 21B, lanes 1, 2). However, when rMKK6 is preincubated with wild-type VopA in the presence of acetyl-CoA, rMKK6 is no longer activated by phosphorylation (Figure 21B, lane 4). By contrast, incubation of the kinase with mutant VopA-C167A has no inhibitory effect on the phosphorylation of rMKK6 (Figure 21B, lanes 5, 6). Although these results demonstrate that VopA can inhibit activation of MKKs by acetylation, they do not explain how VopA is able to inhibit activated MKKs.

VopA Acetylates Four Conserved Residues in MKK6—To determine how VopA is acetylating MKK6, we first assessed the total mass of rMKK6 isolated from bacterial cells expressed either alone (rMKK6) or in the presence of GST-VopA (rMKK6+V) for total mass spectrometric analysis. The mass of rMKK6 is observed as one strong peak at 39,655 kDa, but the mass of rMKK6+V is divided among five peaks, with mass differences in increments of 42 Da, equal to the mass of one acetyl group (Figure 22A). These results indicate that VopA is acetylating four residues on rMKK6.

To determine which four residues of rMKK6 are being modified by GST-VopA, the samples were subjected to LC-MS/MS analyses. No acetylation is observed for rMKK6, whereas rMKK6+V is acetylated on three residues in the activation loop (S207, K210 and T211) and on one residue in the catalytic loop (K172) (Figure 22B) (41). The three residues in the activation loop are the same three residues that are modified by YopJ and, as shown in Figure 22B, the

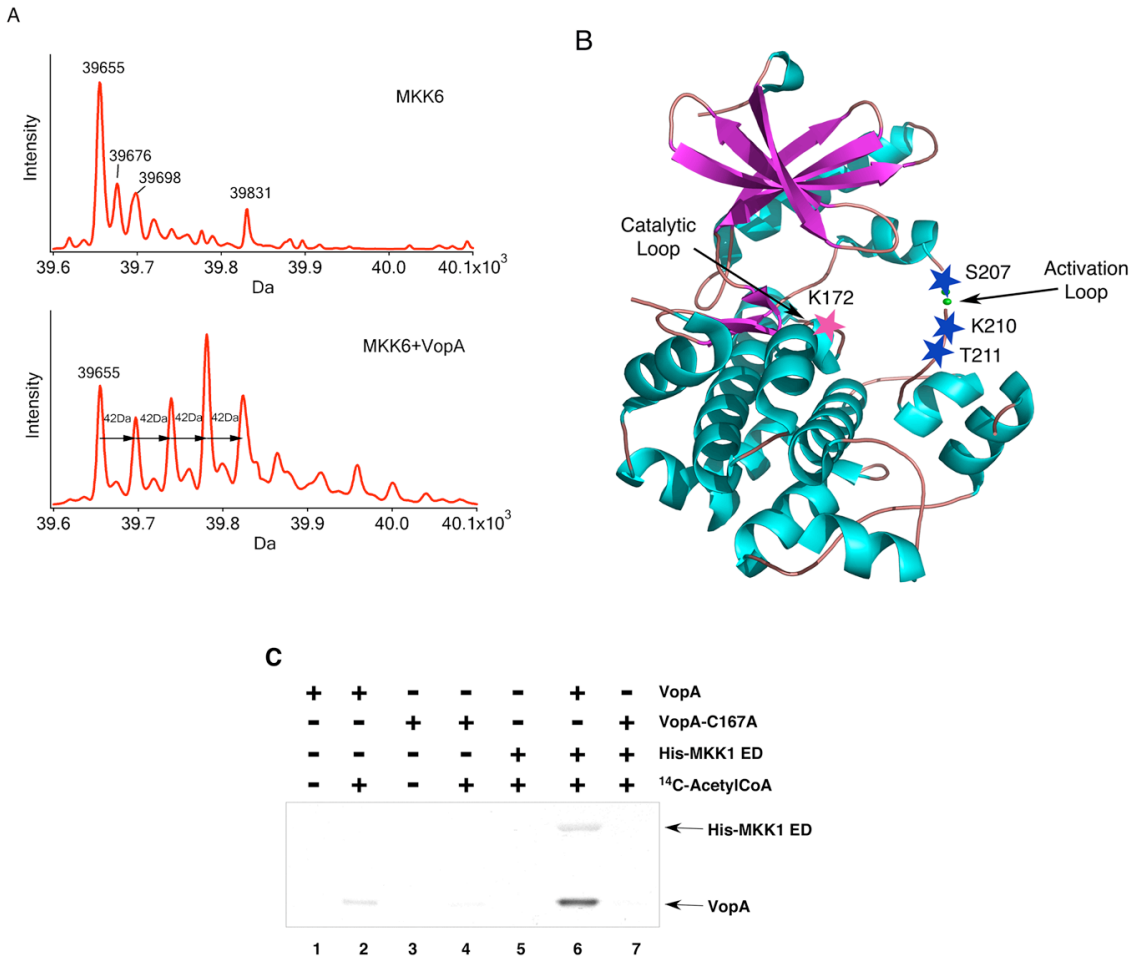

Figure 22: VopA Acetylates the Catalytic Loop of MKK6. *A,* Total mass spectrometric analysis of His-MKK6 expressed in bacteria alone or in the presence of VopA. *B*, Ribbon diagram of the representative kinase structure, MEK1, with modified residues starred. Residues starred in blue are modified by both VopA and YopJ, and the residue starred in pink is only modified by VopA. *C*, VopA acetylates rMKK1. Same as in figure 17(A) except Hisx6-MKK1(S218E, S222D) is used as a substrate. MKK1 ED is Hisx6-MKK1(S218E, S222D)

acetylation by VopA on the activation loop of the kinase directly competes with phosphorylation on the serine and threonine residues. The fourth residue is a conserved lysine that is involved in the coordination of the gamma phosphate of ATP upon nucleotide binding.

To confirm acetylation of the lysine residue on the catalytic loop can occur on an active kinase, we used the purified active phosphomimic, Hisx6-MKK1(S218E, S222D), as a substrate in an acetylation assay (22). We are able to detect acetylation of Hisx6-MKK1(S218E, S222D) by VopA, but not VopA-C167A (Figure 22C). We are also able to detect auto-acetylation of VopA, which is not seen in the assay with rMKK6. This observed difference is likely due to the extended exposure required to see Hisx6-MKK1(S218E, S222D) acetylation (1.5 weeks). The longer exposure time is required because only one acetylation site on Hisx6-MKK1(S218E, S222D) is available for modification, due to the mutations of both serines on the activation loop and the lack of a lysine residue on the activation loop in MKK1.

Acetylation of K172 by VopA Disrupts ATP Binding to MKK—Based on the location of the conserved lysine in the kinase (K172 in MKK6) and its interaction with the gamma-phosphate of ATP, we hypothesized that acetylating this lysine would compromise the binding of ATP, but not ADP, to MKKs. Therefore, we analyzed the binding of the fluorescent nucleotide analogs MANT-ATP and MANT-ADP to constitutively activated Hisx6-MKK1(S218E, S222D). When

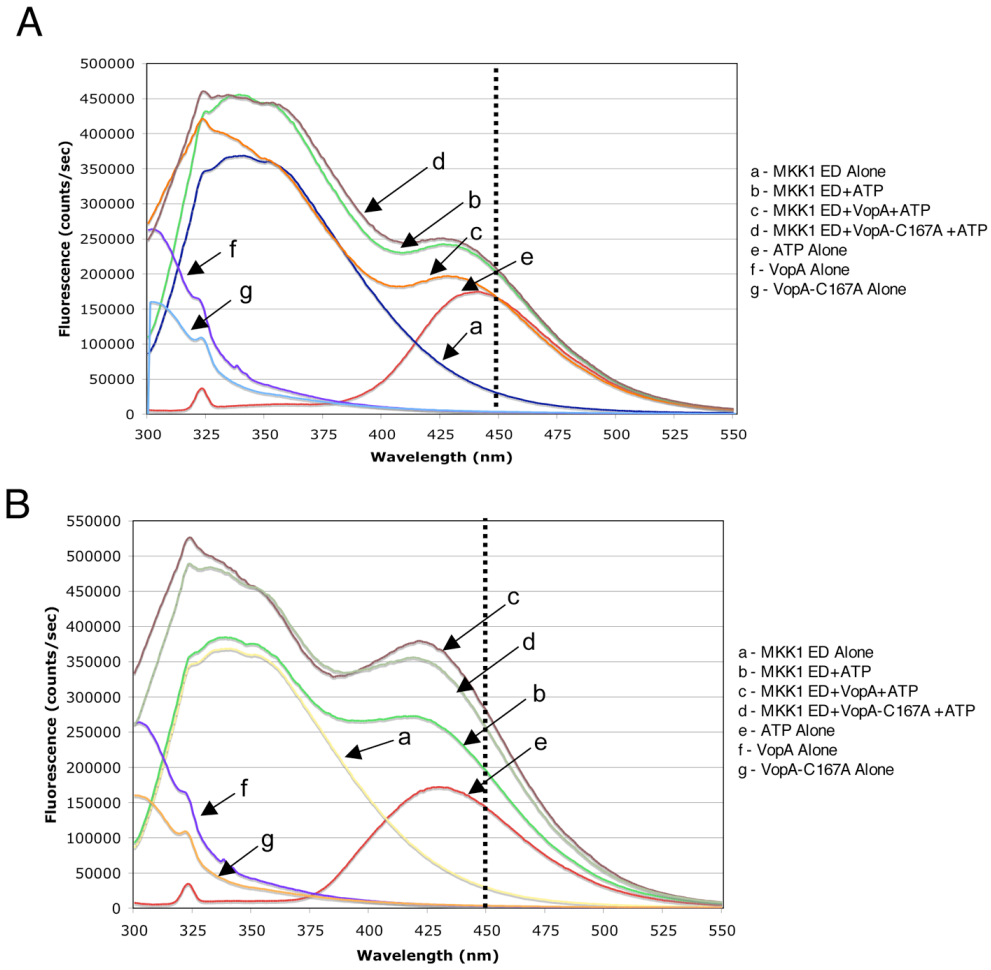

Figure 23: Modification of MKK1 ED disrupts nucleotide binding. *A*, VopA's modification of Hisx6-MKK1(S218E, S222D) disrupts MANT-ATP binding. Hisx6-MKK1(S218E, S222D) (1μM) was preincubated with or without VopA or VopA-C167A (50nM). MANT-ATP (25μM) was added and emission scans measured. MKK1 ED is Hisx6-MKK1(S218E, S222D). *B*, VopA's acetylation of Hisx6-MKK1(S218E, S222D) shows no effect on MANT-ADP binding. Same assay as in *A* except MANT-ADP (25μM) was added.

excited at 290nm the MANT labeled nucleotides, ATP and ADP, emit strong fluorescent peaks (Figure 23A and 23B, respectively) (42). When MANT-ATP or MANT-ADP is incubated with either Hisx6-MKK1(S218E, S222D) or Hisx6-MKK1(S218E, S222D) that was preincubated with VopA-C167A an increase in the emission maximum at ~450nm is observed (Figures 23A and 23B, respectively). This is similar to the emission profile observed for binding of these nucleotide analogs to other kinases (42). However this increase in fluorescence in the presence of MANT-ATP is abrogated when Hisx6-MKK1(S218E, S222D) is preincubated with wild type VopA (Figure 23A). This inhibitory effect is not seen in the presence of MANT-ADP (Figure 23B), although binding of both wild type VopA and VopA-C167A do increase the emission of MANT-ADP bound to Hisx6-MKK1(S218E, S222D). We propose the difference observed with MANT-ATP is attributed to the disruption of the coordination of binding for the gamma phosphate of ATP by the acetylated lysine residue (K192) in MKK1.

Discussion:

Vibrio VopA is an acetyltransferase that modifies MKKs on serine, threonine and lysine. The modification of the lysine residue on the catalytic loop of the kinase is a novel mechanism for inhibiting a kinase. Essentially, VopA uses an acetyl group to nullify the charge on the lysine and destabilize interactions with the gamma phosphate of ATP. The modifications on serine and threonine residues in the active site loop prevent activation of the kinase by

phosphorylation, similar to what has been observed before with *Yersinia* YopJ (1,39). The lysine in the activation loop of the MKK6 is not conserved and, therefore, not thought to be important for the effector's inhibitory activity (1). Based on the architecture of their catalytic site, VopA and other YopJ-like proteins are predicted to transfer the acetyl group from acetyl-CoA to a protein substrate using a ping-pong mechanism (28). For this mechanism, a covalent acetyl-enzyme intermediate is formed that is attacked by the R group of an amino acid. Supported by the presented experiments, VopA must efficiently coordinate two distinct nucleophiles for attack on the acetyl-enzyme intermediate: an amine from a lysine residue or a hydroxyl from a serine or threonine. Although the structure/function studies required to understand the biochemical mechanism used by these enzymes are beyond the scope of this study, from a molecular point of view the mechanism used by this group of enzymes is intriguing and will be interesting to decipher.

Chapter Seven

Infection Studies with *Vibrio parahaemolyticus*

Introduction:

Biochemical analyses have shown that VopA is able to inhibit MAPK signaling pathways in eukaryotic cells, and that VopA utilizes an acetyltransferase activity to acetylate MKKs, which disrupts its activation and its ability to bind ATP. A major question remaining about VopA is what is its role during infection? Is VopA required for virulence? Infection models for *V. parahaemolyticus* have been mostly limited to use of the ligated rabbit ileal loop model and has been mainly used to assess the effects of TDH on tissues (9). However for biochemical studies, a tissue culture model is essential to show direct correlation between infection phenotype and effector mechanism. A more recent study with *V. parahaemolyticus.* examined the effects of the two different TTSSs and used both the rabbit ileal loop model and a tissue culture model of infection (18). In this study it was shown that TTSS1 was required for cytotoxicity in the tissue culture model, and the TTSS2 was required for enterotoxicity in the rabbit ileal loop model of infection. I attempted to develop an infection model to detect TTSS2 activity in a tissue culture. Initial infection studies utilized a panel of *V. parahaemolyticus.* strains obtained from Linda McCarter (U. of Iowa). With these strains I was able to demonstrate that the TTSS1 is required for cytotoxicity but no effect is seen in strains mutant for the TTSS1 and expressing the TTSS2.

These results are similar to that seen in published studies (18). Subsequent studies utilized a panel of strains that were derived from the sequenced RIMD 2210633 strain referred to as the POR strains (18). With these strains I was able to demonstrate a TTSS2-dependent effect in a tissue culture model.

Results and Discussion:

Initial Trial for HeLa Infections—In the published tissue culture studies, HeLa cells were infected with overnight cultures of *V. parahaemolyticus for* 5 hours and observed by phase and fluorescent microscopy. Using these same conditions, I utilized a panel of strains made by Linda McCarter (U. of Iowa) (the LM strains) for my initial infection studies. The wild-type strain is LM5674 a commonly used strain that is deleted for *opaR,* the controller for the switch between opacity and translucence. Deletion of *opaR* locks the strain in the translucent state. It is unknown whether these two states have effects on virulence. Derivatives of the LM5674 strain used in my experiment included LM7029, which is a ΔTTSS1 strain; LM7034, which is a ΔTTSS2 strain; and LM7341, which is a ΔTTSS1 and ΔTTSS2 strain.

For infections, HeLa cells were infected at an MOI of 1 from overnight cultures and incubated for 5 hrs at 37°C. The LM5674 and LM7034 strains killed HeLa cells within the five-hour period (Fig 24 B and D), whereas the LM7029 and LM7341 strains showed no effect on HeLa cells when compared to mock

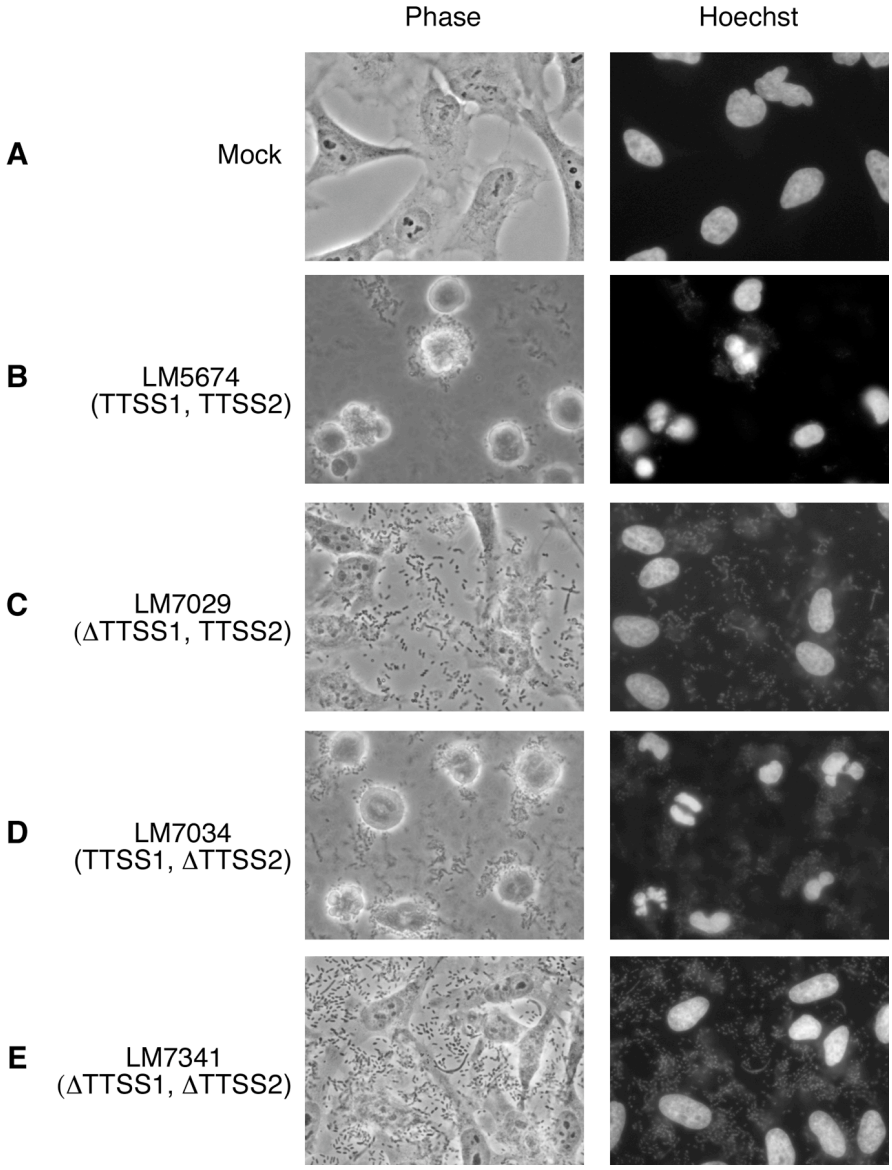

Figure 24: *Vibrio parahaemolyticus* Infections of HeLa Cells. HeLa cells were infected at an MOI of 1 for five hours. Cells were fixed and stained with Hoechst. Cells were viewed by phase and fluorescent microscopy. *A,* Mock. *B,* LM5674, wild-type. *C,* LM7029, TTSS1, ΔTTSS2. *D,* LM7034, ΔTTSS1, TTSS2. *E,* ΔTTSS1, ΔTTSS2

infected cells (Fig 24 A, C and E). All strains were able to replicate to high levels during the infection regardless of their effect on the HeLa cells. These results are consistent with the published results in that there is cytotoxicity with the TTSS1 but the TTSS2 shows no effect on HeLa cells. The lack of an effect by the TTSS2 could be for multiple reasons: 1) the bacterial strains were not induced for secretion of TTSS2 effectors, 2) changes in cell morphology could not be detected by phase microscopy, 3) the TTSS2 could require a specific cell type, 4) bacteria need to be grown under conditions that prime them for infection, and 5) a mutation such as *opaR* could affect secretion of TTSS2 effectors. To overcome these problems I switched to strains derived from a clinical isolate that was used for genomic sequencing (18,31). The conditions for secretion of TTSS effectors had also been defined for these strains (18).

Infection of HeLa Cells with POR Strains—The POR-1 strain is a derivative of the *V. parahaemolyticus* RIMD 2210633 strain, the sequenced strain. The POR-1 strain is deleted for both *tdh* genes present in the genome. Initial characterization of this strain revealed that while the ability to induce fluid accumulation was attenuated in this strain, it was still able to induce cytotoxicity at wild-type levels (31). This indicated an alternate means of virulence. In a subsequent study two derivatives of this strain were made, POR-2 and POR-3; these strains are deleted for the TTSS1 and TTSS2 respectively (18). In this study it was demonstrated that the TTSS1 was required for cytotoxicity and the TTSS2 was required for

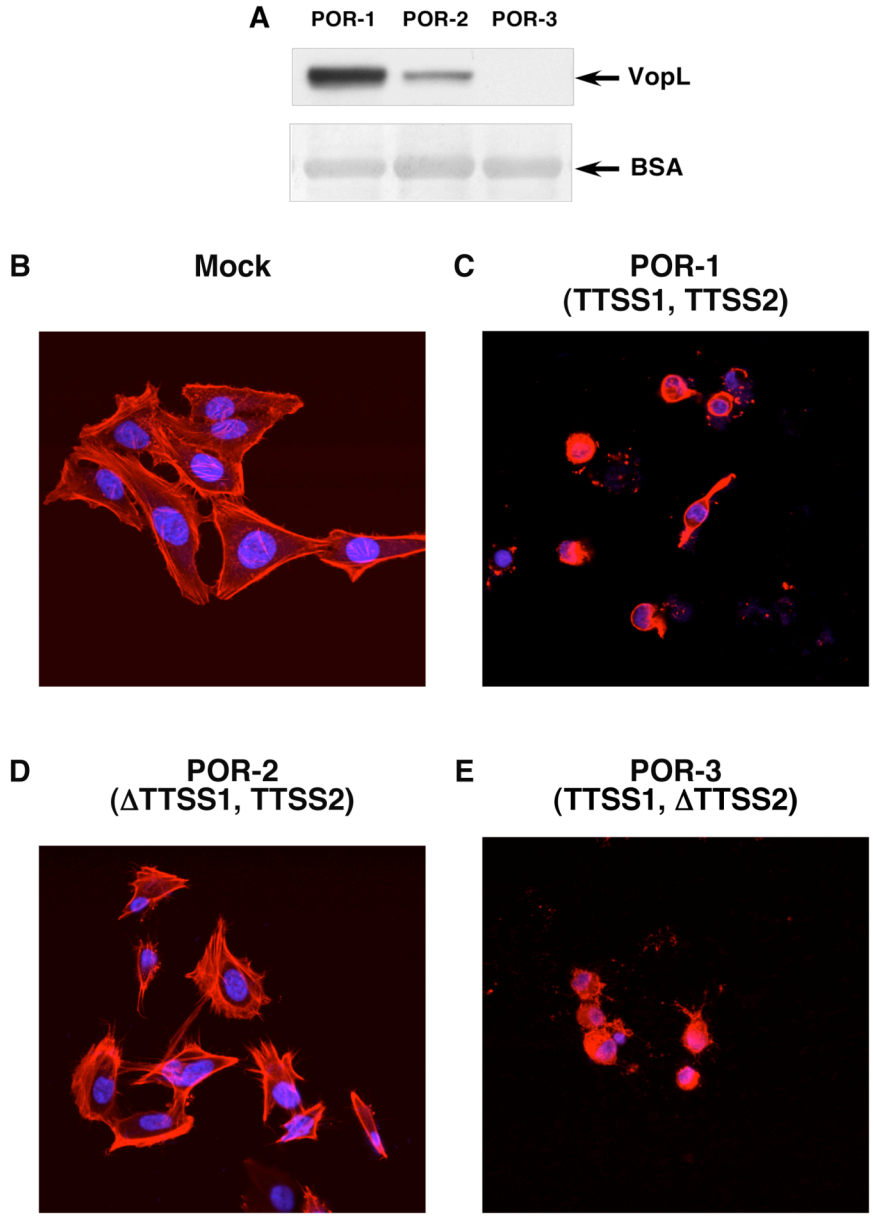

Figure 25: *Characterization of POR strains*. *A,* TCA precipitated samples from POR strains grown in HI for 5hrs showing secretion of VopL, a TTSS2 effector. *B-E,* HeLa cells were infected at an MOI of 10 for two hours. Cells were fixed and stained with Hoechst and rhodamine-phalloidin. Cells were viewed by confocal microscopy. *B,* Mock. *C,* POR-1. *D,* POR-2. *E,* POR-3.

enterotoxicity (18). To verify secretion, strains were grown for five hours in heart infusion media (HI) at 37°C and the filtered culture supernatants were TCA precipitated overnight. Samples were examined by western blot with an anti-VopL, another putative effector secreted by TTSS2. I was able to detect secretion of VopL from POR-1 and POR-2 but not from POR-3 (Fig. 25*A*). This is expected since the POR-3 lacks a functional TTSS2. Attempts to detect secretion of VopA with our polyclonal anti-VopA antibody were unsuccessful, most likely due to the non-specific quality of this antibody.

With secretion from TTSS2 confirmed, I used these strains in infection experiments. Strains were first grown in conditions that induced secretion from TTSS2 (HI for 5 hours at 37°C) and then HeLa cells were infected for 2 hours at an MOI of 10. Cells were fixed and stained with Hoechst and rhodamine-phalloidin and examined by confocal microscopy. The POR-1 and POR-3 strains induced rounding of the HeLa cells and cell death by 2 hours post infection (Fig. 25 B and D). The POR-2 infected HeLa cells had formed stress fibers and were beginning to pull away from the plate (Fig. 25 C). These results indicate that the TTSS2 can be studied in a tissue culture model of infection. However, the effects of the TTSS2 are masked by the potency of the TTSS1, and the phenotype requires the preinduction of the TTSS2.

Some evidence exists to confirm that the phenotypes are a result of TTSS2 function. Studies with the VopL knockout indicate that VopL plays a role in the

induction of stress fiber formation during infection (Liverman, et al. in press). There are also two other potential effectors that could induce cytoskeleton rearrangements, VPA1321 and VPA1327. VPA1321 is a homologue of the *E. coli* toxin cytotoxic necrotizing factor-1 (CNF-1), which inhibits Rho, Rac and CDC42 function in cells. VPA1327 is a homologue of the *Pseudomonas* effector ExoT, which is as an ADP-ribosyltransferase targeting the focal adhesion complex. This trio of effectors could serve to disrupt epithelial barriers during infections. VopA could complement these effectors by attenuating the innate immune response and could also function to inhibit cytoskeletal signaling by MAPK pathways that are involved in this process.

Chapter Eight

Discussion

Until recently very little was known about the pathogenesis of *V. parahaemolyticus.,* previous studies had been limited to understanding the function of the thermostable direct hemolysin, which until the genome was sequenced, was used as a marker for pathogenicity. With the discovery of the two TTSSs within the genome, studies on the functions of type III effectors became essential for broadening the understanding of *V. parahaemolyticus.* infection. Some published studies have already established that the TTSS2 is required for virulence in the rabbit ileal loop model of infection while the TTSS1 is required for cytotoxicity in a tissue culture model. A better understanding of mechanisms utilized by the type III effectors secreted by the TTSS2 will lead to a more complete understanding of how *V. parahaemolyticus.* induces an infection. This dissertation has focused on the characterization of VopA, one of the first identified type III effectors in *V. parahaemolyticus.*

VopA Inhibits MAPK Signaling in Eukaryotic Cells

Due to the homology of VopA to YopJ, initial studies focused on VopA's potential effects on signaling pathways. YopJ was known to inhibit both MAPK and NFκB signaling in eukaryotic cells (43). Transfection assays demonstrated that unlike YopJ, VopA only inhibits MAPK signaling and shows no effect on NFκB signaling (40). These results are not unprecedented; another homologue of

YopJ, AvrA from *Salmonella* is specific for the NFκB pathway (32). Each of these pathogens has taken this type of effector and altered the function to fit the needs of the bacteria during infection.

VopA also utilizes an evolutionarily conserved mechanism since like YopJ, VopA is able to inhibit MAPK signaling in yeast. In addition to the inhibition of MAPK signaling VopA also induces a growth arrest phenotype in yeast. This is in contrast to YopJ, which shows no effect on yeast growth (40). The difference in phenotype hints at the likelihood for additional targets for VopA in the cell, but the phenotype itself does not give directs hints as to what the targets could be. A growth arrest phenotype is a very broad phenotype and can be caused by many different types of effects including cell cycle arrest and effects on metabolism.

VopA's Targets in Cells

Binding partners for YopJ were identified by a yeast two-hybrid screen and verified by GST pulldowns and identification of these binding partners also helped to identify the function of YopJ in the cell (22). The binding partners of YopJ have since been identified as the catalytic targets of YopJ. Unfortunately a similar yeast two-hybrid screen using VopA as bait did not recover any potential binding partners. We had already shown that VopA could inhibit MAPK signaling, but the question still remained as to how. Given the specificity of YopJ

for its target we hypothesized that VopA was targeting a component of the MAPK pathway.

To continue searching for binding partners two different types of biochemical purification were utilized, GST-pulldowns and TAP-tag purification. Purification of TAP-VopA resulted in purified VopA but no additional proteins. Although the purification was performed with multiple salt conditions to rule out disruption of potential complexes, there were no binding partners isolated. The TAP-VopA construct used in this experiment was an overexpression construct, so the expression level of TAP-VopA was significantly higher than the expression of any potential binding partners. Therefore, the lack of a positive result could have been due to a detection issue. Previous studies using TAP-tag purification have been with tagged proteins expressed from their native promoter, and therefore the expression level of the tagged protein did not overwhelm the expression levels of other members of the complex. Since VopA is not a native protein this was not an option.

The GST pulldowns unlike the TAP-tag purification did identify a potential binding partner, filamin. Initially, filamin was speculated to be a good potential binding partner, because it is an actin cross linking protein that is involved in the formation of actin webs and the integration of signaling related to cytoskeletal rearrangements (38). In addition, Filamin has been shown to interact with SEK-1 and TRAF2 (38,44). Both of these proteins are involved in the

activation of Jnk signaling. SEK-1 is also known as MKK4 and is the MKK equivalent in the Jnk pathway (44). VopA has been shown to modify the MKKs from the p38 and ERK pathways (MKK6 and MKK1, respectively); this indicates that SEK-1 is the most likely target for VopA in the Jnk pathway. Since filamin can serve as a scaffolding protein for this signaling cascade (44), it would make sense that VopA would be able to interact with filamin. However attempts to coimmunoprecipitate filamin and VopA from mammalian cells using an anti-filamin antibody were unsuccessful. Perhaps a more direct test of binding, such as with purified proteins would yield a different result. It is difficult to discount the potential of filamin as a VopA binding partner given the role it plays in coordinating signaling pathways known to be inhibited by VopA.

VopA functions as a Dual Specific Acetyltransferase

I have demonstrated that VopA acetylates the critical serine and threonine in the activation loop of MKKs similar to YopJ. In addition, I have shown that VopA is also able to acetylate a critical lysine residue in the catalytic loop. This lysine is conserved in all kinases and is involved in the coordination of the γ-phosphate of ATP. Acetylation of this lysine disrupts ATP binding, thereby allowing VopA to inhibit activated kinases. This is a mechanism distinct from that observed for YopJ.

VopA is an Ideal Molecular Inhibitor

For decades, scientists have been, and still are, trying to design specific inhibitors that target the nucleotide-binding site of kinases. Attempts to make selective inhibitors, such as imatinib, have been focused on targeting the inactive state of a kinase because of its unique fold (45). In their active states many kinases conform to a canonical structure, which makes it difficult to target a specific kinase or even a family of kinases. Natural selection has once again proven to be the champion chemist by creating VopA. This bacterial effector disrupts not only the inactive form of the kinase but the active form as well. A greater understanding of the interactions between VopA and its substrate might lead to the ability to dissect the acetylation of the active kinase versus the inactive kinase and allow for the development of a more selective class of inhibitors.

VopA efficiently inhibits the MKKs in two ways by targeting different sites on the kinase. First, VopA targets the pharmacological 'sweet spot' (nucleotide binding site) of a kinase by masking the charge on a lysine residue with an acetyl moiety. This change in charge and shape of the nucleotide-binding pocket of a kinase drastically changes the activity of the enzyme. The modified kinase is no longer able to bind ATP, but is still able to bind ADP. Therefore, acetylated MKKs are covalently locked into an inactive state and are no longer able to modify their substrates. VopA also targets the activation of the MKKs by acetylation of the activation loop on the serine and threonine residues, directly

competing with phosphorylation, resulting in a kinase that cannot be activated. Perhaps, it is understandable that VopA appears to be a more potent inhibitor of MAPK signaling than YopJ, because VopA is able to inactivate MKKs by two mechanisms whereas YopJ only uses one (40).

Recently another effector, the *Yersinia* kinase YpkA has been shown to block the binding of a GTP to the G-protein Gαq. In contrast to VopA that modifies the nucleotide binding site with a neutral acetyl group, YpkA phosphorylates a serine residue, found in the proximity of the GTP binding site (46). Phosphorylation of Ser47 on Gαq is predicted to reduce its affinity for GTP, thereby inactivating the G-protein. The molecular mechanisms are quite distinct for these two effectors but the global outcome is the same: they disrupt the binding of nucleotide to a host enzyme.

Diversity of Acetyltransferase Effector Family

Bacterial effectors, much like viral oncoproteins, target and manipulate host signaling by usurping or mimicking a host activity (28). The bacterial effectors contain a variety of enzymatic activities that includes hydrolases, phosphatases, GAPs, GEFs and kinases (15,28,46). Recently, another enzyme, a serine/threonine acetyltransferase was observed and now, an enzyme has been observed to use lysine acetylation to manipulate host signaling (1,28,39,47). Some of these effectors, like VopA, belong to a large family of effectors that are expressed by a variety of pathogens (40,48). These families are arranged by the

homology found in their primary amino acid sequence. As with other families of enzymes, the molecular activity of a bacterial effector can be predicted based on the biochemical activity of one or more of the family members. Proving an effector has the predicted activity requires direct biochemical experiments.

Even though the substrates of many eukaryotic enzymes can be predicted due to the conservative nature of signaling pathways throughout evolution, the identification of substrates for bacterial effectors is challenging, to say the least. These enzymes have been mutated and molded over time to contain an activity that is custom designed by the pathogen that expresses it. For example, *Yersinia* YopJ cripples the innate immune response by inhibiting all MAPK pathways and the NFκB pathway, whereas, *Vibrio* VopA targets only MAPK pathways, albeit, in a more potent manner (22,40). Homologues of these acetyltransferases expressed by *Rhizobium*, a plant symbiont, may use this activity to attenuate host signaling pathways to facilitate a commensal relationship between the bacteria and host (15,22). Finally plant pathogens seem to be the most aggressive with regard to this family of effectors because some of the bacteria that target plants contain over a half-dozen genes encoding YopJ-like effectors (49).

Modification of a protein with lysine acetylation is a reasonable way to regulate the nucleotide binding to a kinase because lysine acetylation, like phosphorylation, is reversible. We propose that VopA exemplifies an effector that usurped the eukaryotic activity of lysine acetylation. Consistent with this

hypothesis is the observation that expression of VopA in yeast suspends cell growth, but the growth suppression can be reversed when expression of VopA is stopped. In addition, these observations support, by inference, that O-acetylation (serine and threonine acetylation), like N-acetylation (lysine acetylation) will be reversible. Therefore, serine, threonine and lysine acetylation might be reversible posttranslational modifications that are used to modulate the enzymatic activity of eukaryotic signaling machinery.

Specificity of YopJ Proteins

YopJ proteins possess a unique inhibitory profile. Based on these profiles it would appear that each molecule also has a unique set of cellular targets. However, I have found that VopA and YopJ both modify the same target in the MAPK pathway, MKK. Why then is VopA specific for the MAPK pathway and YopJ able to inhibit both the NFκB and the MAPK pathways? Unfortunately structural data for these proteins is unavailable so a direct analysis of potential binding pockets is not possible. A panel of PBS2 mutants though has proved a useful tool in understanding this problem. PBS2 is the MKK in the yeast HOG pathway. A screen of PBS2 mutants that suppress the YopJ phenotype allowed for mapping of the YopJ binding site on the kinase. One of the PBS2 mutants had a mutation in the G-helix of the kinase and was no longer able to interact with YopJ via two-hybrid assay (Hao et al, submitted). When this PBS2 mutant was tested with VopA, it was unable to suppress VopA's inhibition of the HOG pathway.

These results indicate that the binding site is not shared between these two bacterial effectors and may provide insight into the specificity of these effector proteins.

Future Directions

Enzymology of VopA

I have shown that VopA is an acetyltransferase targeting MKKs, but questions still remain as to the actual mechanism of acetylation, the affinity of VopA for its substrate, and the kinetic parahaemolyticusmeters of this enzyme. Experiments are currently being conducted to develop a quantitative *in vitro* enzyme assay. A quantitative enzyme assay would be able to address these questions through application of classic kinetics analysis. The ongoing experiments are utilizing radioactively labeled acetyl-CoA as a substrate and measuring the transfer of radioactivity to the substrate.

Identification of New Targets

VopA's specificity for the MAPK signaling pathways in eukaryotic cells compared to YopJ, which inhibits two different pathways would appear to imply that VopA is a more specific enzyme and might not have any other targets in the cell. However, the growth arrest induced by VopA in yeast would imply other targets in the cell not shared by YopJ.

Attempts to define additional targets of VopA targets have not yielded results. This could be due to detection issues or due to binding affinity of VopA

for its targets. With the identification of VopA as an acetyltransferase the hunt for targets can be carried out in a less stringent manner by using modified acetyl-CoA substrates that fluorescently label modified target proteins.

Infection Models

My infection studies indicate that both TTSSs can be examined in a tissue culture model of infection. However the effects of the TTSS1 mask the effects of TTSS2. Infection with a TTSS1 knockout demonstrates that the TTSS2 has interesting effects on tissue culture cells. The most obvious effect is the induction of actin stress fibers in the cell. Based on homology and published results there are several candidates for induction of this phenotype including VPA1327, the CNF-1 homologue, VopT (VPA1327), which has been shown to ribosylate Ras (23), and VopL (VPA1370), which has been shown to induce the formation of actin fibers both *in vitro* and *in vivo* (Liverman, et al, in press). Infection studies with knockout strains of these three potential effectors will be useful for dissecting the contributions of identified effectors during infection. Further studies would also include studies with VopA knockout strains to determine if VopA inhibits signaling upon translocation. VopA's effect on signaling pathways during infection has been observed using a heterologous infection system with *Yersinia pseudotuberculosis*. VopA is able to complement the inhibition of MAPK signaling in a YopJ deletion mutant (Chapter 6).

Future studies with *V, parahaemolyticus.* strains, including the VopA knockout, will be important for understanding the pathogenesis of *V. parahaemolyticus.,* and how the two TTSSs are utilized by this pathogen. There are two possible models. In the first model the two TTSSs work independently of each other. The TTSS1 is used in the environment to defend itself against potential predators such as amoeba or to establish itself in a commensal relationship. The TTSS2 is then used during infection of humans. In the second model, the two TTSSs would work together. The TTSS2 disrupts epithelial barriers by manipulating the actin cytoskeleton, which allows the bacteria to disseminate and engage the TTSS1, which could induce cytotoxicity in tissues. A better understanding of these mechanisms would allow for better methods of treating this disease, which is becoming more common throughout the world.

References

1. Mukherjee, S., Keitany, G., Li, Y., Wang, Y., Ball, H. L., Goldsmith, E. J., and Orth, K. (2006) *Science* **312**(5777), 1211-1214

2. Joseph, S. W., Colwell, R. R., and Kaper, J. B. (1982) *Crit Rev Microbiol* **10**(1), 77-124

3. Makino, K., Oshima, K., Kurokawa, K., Yokoyama, K., Uda, T., Tagomori, K., Iijima, Y., Najima, M., Nakano, M., Yamashita, A., Kubota, Y., Kimura, S., Yasunaga, T., Honda, T., Shinagawa, H., Hattori, M., and Iida, T. (2003) *Lancet* **361**(9359), 743-749

4. Panina, E. M., Mattoo, S., Griffith, N., Kozak, N. A., Yuk, M. H., and Miller, J. F. (2005) *Mol Microbiol* **58**(1), 267-279

5. Morris, J. G., Jr. (2003) *Clin Infect Dis* **37**(2), 272-280

6. McCarter, L. (1999) *J Mol Microbiol Biotechnol* **1**(1), 51-57

7. McCarter, L. L. (2004) *J Mol Microbiol Biotechnol* **7**(1-2), 18-29

8. Daniels, N. A., MacKinnon, L., Bishop, R., Altekruse, S., Ray, B., Hammond, R. M., Thompson, S., Wilson, S., Bean, N. H., Griffin, P. M., and Slutsker, L. (2000) *J Infect Dis* **181**(5), 1661-1666

9. Nishibuchi, M., and Kaper, J. B. (1995) *Infect Immun* **63**(6), 2093-2099

10. Fabbri, A., Falzano, L., Frank, C., Donelli, G., Matarrese, P., Raimondi, F., Fasano, A., and Fiorentini, C. (1999) *Infect Immun* **67**(3), 1139-1148

11. Fukui, T., Shiraki, K., Hamada, D., Hara, K., Miyata, T., Fujiwara, S., Mayanagi, K., Yanagihara, K., Iida, T., Fukusaki, E., Imanaka, T., Honda, T., and Yanagihara, I. (2005) *Biochemistry* **44**(29), 9825-9832

12. Lin, Z., Kumagai, K., Baba, K., Mekalanos, J. J., and Nishibuchi, M. (1993) *J Bacteriol* **175**(12), 3844-3855

13. Nair, G. B., Ramamurthy, T., Bhattacharya, S. K., Dutta, B., Takeda, Y., and Sack, D. A. (2007) *Clin Microbiol Rev* **20**(1), 39-48

14. Ghosh, P. (2004) *Microbiol Mol Biol Rev* **68**(4), 771-795

15. Viboud, G. I., and Bliska, J. B. (2005) *Annu Rev Microbiol* **59**, 69-89

16. Schlumberger, M. C., and Hardt, W. D. (2006) *Curr Opin Microbiol* **9**(1), 46-54

17. Ono, T., Park, K. S., Ueta, M., Iida, T., and Honda, T. (2006) *Infect Immun* **74**(2), 1032-1042

18. Park, K. S., Ono, T., Rokuda, M., Jang, M. H., Okada, K., Iida, T., and Honda, T. (2004) *Infect Immun* **72**(11), 6659-6665

19. Schmidt, H., and Hensel, M. (2004) *Clin Microbiol Rev* **17**(1), 14-56

20. Fasano, A., and Nataro, J. P. (2004) *Adv Drug Deliv Rev* **56**(6), 795-807

21. Deng, Q., Sun, J., and Barbieri, J. T. (2005) *J Biol Chem* **280**(43), 35953-35960

22. Orth, K., Palmer, L. E., Bao, Z. Q., Stewart, S., Rudolph, A. E., Bliska, J. B., and Dixon, J. E. (1999) *Science* **285**(5435), 1920-1923

23. Kodama, T., Rokuda, M., Park, K. S., Cantarelli, V. V., Matsuda, S., Iida, T., and Honda, T. (2007) *Cell Microbiol*

24. Orth, K., Xu, Z., Mudgett, M. B., Bao, Z. Q., Palmer, L. E., Bliska, J. B., Mangel, W. F., Staskawicz, B., and Dixon, J. E. (2000) *Science* **290**(5496), 1594-1597

25. Yoon, S., Liu, Z., Eyobo, Y., and Orth, K. (2003) *J Biol Chem* **278**(4), 2131-2135

26. Li, S. J., and Hochstrasser, M. (1999) *Nature* **398**(6724), 246-251

27. Xia, Z. P., and Chen, Z. J. (2005) *Sci STKE* **2005**(272), pe7

28. Mukherjee, S., Hao, Y. H., and Orth, K. (2007) *Trends Biochem Sci* **32**, 210-216

29. Vojtek, A. B., and Hollenberg, S. M. (1995) *Methods Enzymol* **255**, 331-342

30. Palmer, L. E., Hobbie, S., Galan, J. E., and Bliska, J. B. (1998) *Mol Microbiol* **27**(5), 953-965

31. Park, K. S., Ono, T., Rokuda, M., Jang, M. H., Iida, T., and Honda, T. (2004) *Microbiol Immunol* **48**(4), 313-318

32. Collier-Hyams, L. S., Zeng, H., Sun, J., Tomlinson, A. D., Bao, Z. Q., Chen, H., Madara, J. L., Orth, K., and Neish, A. S. (2002) *J Immunol* **169**(6), 2846-2850

33. Beg, A. A., and Baltimore, D. (1996) *Science* **274**(5288), 782-784

34. Van Antwerp, D. J., Martin, S. J., Kafri, T., Green, D. R., and Verma, I. M. (1996) *Science* **274**(5288), 787-789

35. Harrison, J. C., Zyla, T. R., Bardes, E. S., and Lew, D. J. (2004) *J Biol Chem* **279**(4), 2616-2622

36. Sun, J., Hobert, M. E., Rao, A. S., Neish, A. S., and Madara, J. L. (2004) *Am J Physiol Gastrointest Liver Physiol* **287**(1), G220-227

37. Rigaut, G., Shevchenko, A., Rutz, B., Wilm, M., Mann, M., and Seraphin, B. (1999) *Nat Biotechnol* **17**(10), 1030-1032

38. Stossel, T. P., Condeelis, J., Cooley, L., Hartwig, J. H., Noegel, A., Schleicher, M., and Shapiro, S. S. (2001) *Nat Rev Mol Cell Biol* **2**(2), 138-145

39. Mittal, R., Peak-Chew, S. Y., and McMahon, H. T. (2006) *Proc Natl Acad Sci U S A* **103**(49), 18574-18579

40. Trosky, J. E., Mukherjee, S., Burdette, D. L., Roberts, M., McCarter, L., Siegel, R. M., and Orth, K. (2004) *J Biol Chem* **279**(50), 51953-51957

41. Ohren, J. F., Chen, H., Pavlovsky, A., Whitehead, C., Zhang, E., Kuffa, P., Yan, C., McConnell, P., Spessard, C., Banotai, C., Mueller, W. T., Delaney, A., Omer, C., Sebolt-Leopold, J., Dudley, D. T., Leung, I. K., Flamme, C., Warmus, J., Kaufman, M., Barrett, S., Tecle, H., and Hasemann, C. A. (2004) *Nat Struct Mol Biol* **11**(12), 1192-1197

42. Aubol, B. E., Nolen, B., Shaffer, J., Ghosh, G., and Adams, J. A. (2003) *Biochemistry* **42**(44), 12813-12820

43. Orth, K. (2002) *Curr Opin Microbiol* **5**(1), 38-43

44. Marti, A., Luo, Z., Cunningham, C., Ohta, Y., Hartwig, J., Stossel, T. P., Kyriakis, J. M., and Avruch, J. (1997) *J Biol Chem* **272**(5), 2620-2628

45. Nagar, B., Hantschel, O., Young, M. A., Scheffzek, K., Veach, D., Bornmann, W., Clarkson, B., Superti-Furga, G., and Kuriyan, J. (2003) *Cell* **112**(6), 859-871

46. Navarro, L., Koller, A., Nordfelth, R., Wolf-Watz, H., Taylor, S., and Dixon, J. E. (2007) *Mol Cell* **26**(4), 465-477

47. Morrison, D. K. (2001) *J Cell Sci* **114**(Pt 9), 1609-1612

48. Staskawicz, B. J., Mudgett, M. B., Dangl, J. L., and Galan, J. E. (2001) *Science* **292**(5525), 2285-2289

49. Altschul, S. F., Madden, T. L., Schaffer, A. A., Zhang, J., Zhang, Z., Miller, W., and Lipman, D. J. (1997) *Nucleic Acids Res* **25**(17), 3389-3402

VITAE

Jennifer Elizabeth Trosky was born in Austin, Texas, on June 19, 1980, the daughter of Paula Kay Murr Trosky and James Glenn Anthony Trosky. After graduating from the Oklahoma School of Science and Mathematics, Oklahoma City, Oklahoma, in 1998, she began attending Regis University in Denver. Colorado. During the summer of 2001 she participated in the Summer Undergraduate Research Fellowship program (SURF) at University of Texas Southwestern Medical Center at Dallas. She received a Bachelor of Science degree with majors in Honors-in-Biochemistry and Mathematics from Regis University in 2002. She entered the graduate program at the University of Texas Southwestern Medical Center at Dallas and entered Kim Orth's lab in the spring of 2003. Following graduation in September, 2007 she will move on to a postdoctoral fellowship at Stanford University in the lab of Dr. David Relman. Moving with her will be her new husband, Horacio Dinalo. They married on May 4, 2007.

Permanent Address: 30103 S. 4230 Rd.
Inola, OK 74036